AI-AEC-13102
NASA-CR-121230

MATERIALS INTERACTIONS BETWEEN THE THERMOELECTRIC CONVERTER AND THE 5-kwe REACTOR SYSTEM

AEC Research and Development Report

Atomics International Division
Rockwell International

P.O. Box 309
Canoga Park, California 91304

AI-AEC-13102
SNAP REACTOR
SNAP PROGRAM
M3679-R69
C-92b
NASA-CR-121230

MATERIALS INTERACTIONS BETWEEN THE THERMOELECTRIC CONVERTER AND THE 5-kwe REACTOR SYSTEM

P. B. FERRY

Atomics International Division
Rockwell International

P.O. Box 309
Canoga Park, California 91304

CONTRACT: AT(04-3)-701
ISSUED: JUNE 30, 1973

FOREWORD

The work described here was done at the Atomics International Division of Rockwell International Corporation, under the direction of the Space Nuclear Systems Division, a joint AEC-NASA office. Project management was provided by NASA-Lewis Research Center and the AEC-SNAP Project Office.

DISTRIBUTION

This report has been distributed according to the category "Systems for Nuclear Auxiliary Power (SNAP) Reactor – SNAP Program," as given in the Standard Distribution for Classified Scientific and Technical Reports, M-3679, and according to the NASA Supplementary Report Distribution List at the end of this report.

CONTENTS

TABLES

FIGURES

FIGURES

ABSTRACT

Integration of a compact thermoelectric converter with the 5-kwe reactor system requires introduction of Ta - 10 W piping into some portion of the primary coolant loop. The accompanying material interaction uncertainties could affect the present system design. These include degradation of the required austenitic - refractory metal transition joint during operation at high temperatures, loss of corrosion resistance, embrittlement by the presence of hydrogen, and loss of design margin by transport of interstitial elements. Analysis and limited experimental evidence indicates that these potential materials interactions can be adequately controlled. It appears that the Group Va refractory metal can be utilized without unacceptable adverse effect on system reliability.

I. INTRODUCTION

The power conversion scheme for the 5-kwe compact reactor system consists of a series of modular heat exchangers containing thermoelectric material. Figure 1 shows the overall arrangement of the system. Heat is provided to the thermoelectric power converter from the zirconium hydride fuel by the alkali metal coolant, NaK. The thermal gradient is provided by the colder, secondary loop. Heat is rejected from this loop by radiation to space. Figure 2 shows some of the details of the power converter module, which produces 322 w and weighs only 13 lb. The compact geometry is achieved by arranging, within a counterflow heat exchanger, all the thermoelectric material, along with all of the electrical contacts, insulators, diffusion barriers, etc. The thermal gradient required to drive the thermoelectric material in such a small volume is produced by the high efficiency of the liquid metal heat transfer medium.

The temperature difference between the two loops, and therefore across the modified lead telluride thermoelectric material, is ~650°F. The primary coolant loses, and the secondary gains, ~100°F during their transit through the module. The temperature of the primary loop will increase, as accompanying technology allows, in order to increase the efficiency of the device. Within the past few years, the demonstrated operating temperature has risen to as high as 1225°F. A more reasonable average operating temperature for demonstrated, reliable, long-term operation appears to be 1100°F.

One of the problems associated with a high-power-density heat exchanger is the high stresses induced as a result of differential thermal expansion. During normal operation, there are significant thermal gradients within the structure; although, at times (e.g., prior to startup or during shutdown), the structure becomes essentially isothermal. This variation in temperature gradient operation results in significant stresses and strains.

There were significant power losses in operation of early models of the compact module. Evaluation of the assemblies indicated that the bulk of the loss was due to the distortion caused by differential movement within the

Figure 1. 5-kwe Reactor System

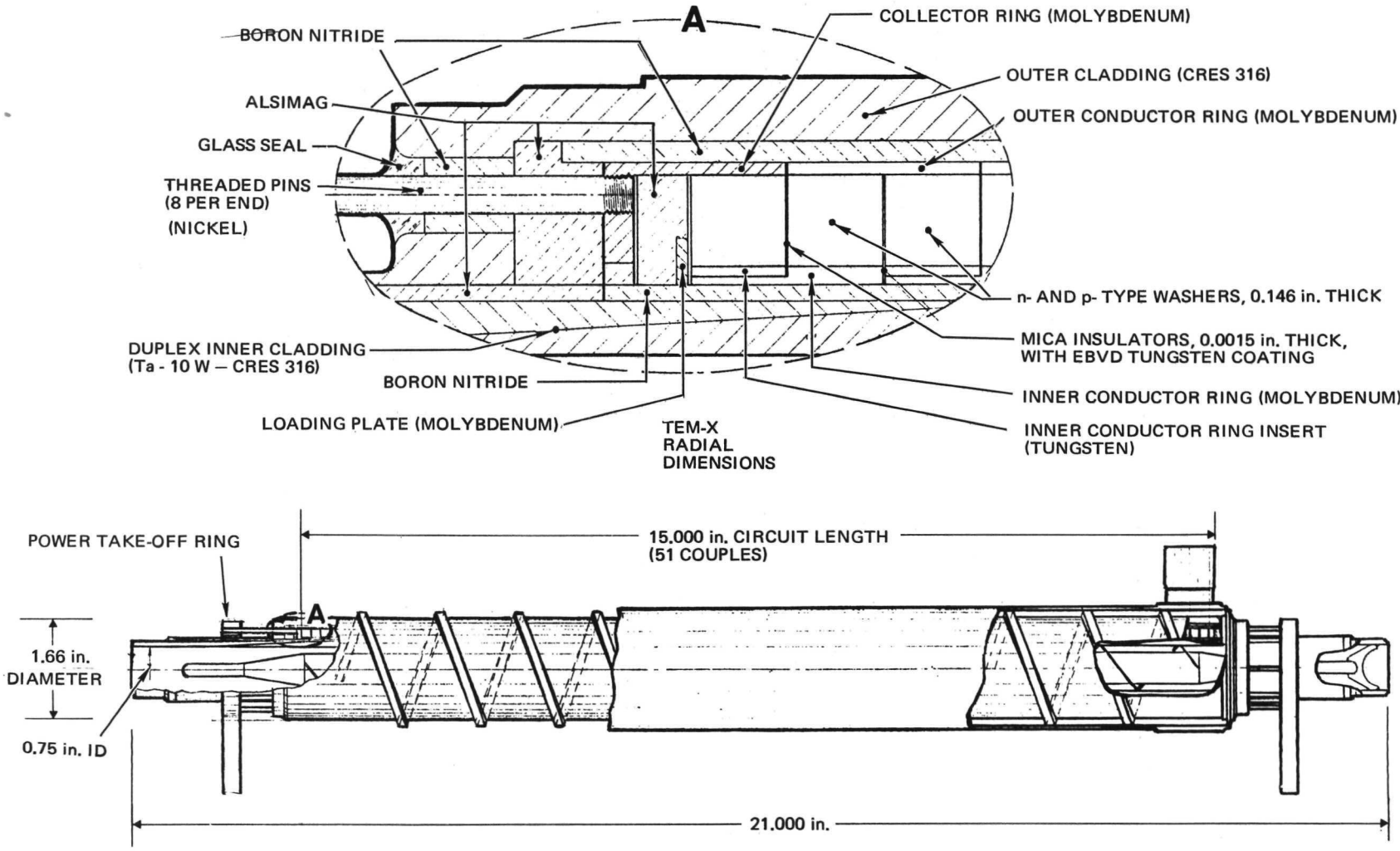

Figure 2. Module Power–5-kwe System, Conceptual Design

assembly. A number of design schemes were evaluated for solution of the problem, but none proved to be very satisfactory. The solution was to eliminate the differential movement by providing a material of high thermal expansion for low-temperature regions of the heat exchanger, and a low-expansion material for the high-temperature portions. To minimize perturbations to the system, a major effort was made to retain the conventional austenitic construction alloys and established fabrication techniques. The solution is shown in Figure 2. The initial inner, primary, hot-leg austenitic steel pipe was replaced with a refractory metal Ta - 10 W. The alloy has adequate strength, is compatible with NaK, can be reliably joined to the AISI Type 316 stainless steel piping, and has a thermal expansion coefficient less than half that of the steel. Modules were fabricated, thermal cycled, and operated for times as long as 14,000 hr at an average temperature of 1085°F, without serious degradation of the power conversion efficiency. (1)

The introduction of a Group Va refractory metal to the primary system of the reactor does, however, introduce some additional uncertainties into reliable reactor system operation. These include: (1) degradation of the transition joint, (2) loss of corrosion resistance in the piping, (3) embrittlement by exposure to hydrogen, and (4) change in design properties, as a result of transport of interstitial elements from other structural members in the system. A program was undertaken to evaluate these uncertainties, as well as to uncover any others which might occur as a result of introducing the new alloy into the primary reactor coolant. This program identified potential problems, analyzed their potential effect on system reliability and performance, and recommended and carried out experimental work, where required by lack of existing applicable experience. At the time the reactor system contract was closed out (prior to completion of the program), a major portion of the analytical work had been completed, and experimental work had progressed to where feasibility questions had been answered. This report relates a summary of both the analytical and experimental portions of the program.

II. OPERATIONAL UNCERTAINTIES

A. DEGRADATION OF TRANSITION JOINT

A number of approaches have been made toward developing a reliable, structurally sound, and leak-proof transition between refractory metals and nickel- and iron-base structural materials for elevated-temperature operation. Of these, the best developed and most reliable processes are: direct coextrusion, explosive bonding, diffusion bonding, and brazing. The coextrusion approach was selected for this design application.

The joints were produced by hot-tandem coextruding Ta - 10 W and AISI Type 316 stainless steel, canned in mild steel for protection from contamination. Figure 3 shows the configuration of the finished joint. The hot forging received during the extrusion produces a bond between the two materials, up to temperatures exceeding 1300°F.[2]

Further tests have shown that, at low temperatures, this bond remains stable, and one should expect long-term, reliable service. A number of programs have shown that diffusion takes place between tantalum-, nickel-, and iron-base alloys. Two independent programs evaluated both diffusion and

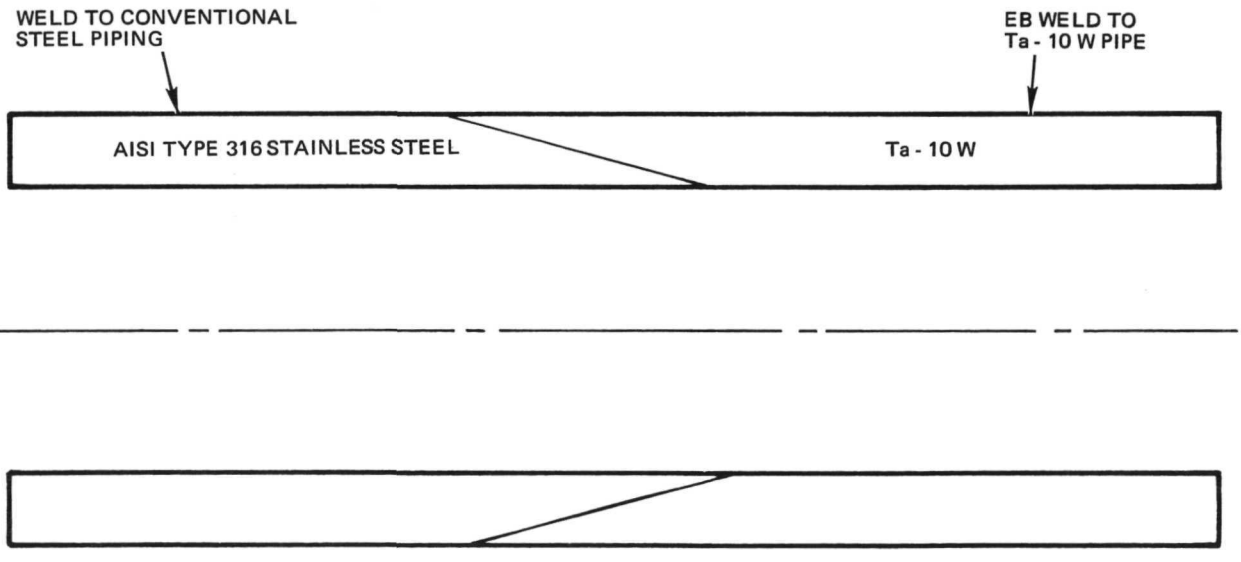

Figure 3. Design of Transition Joint

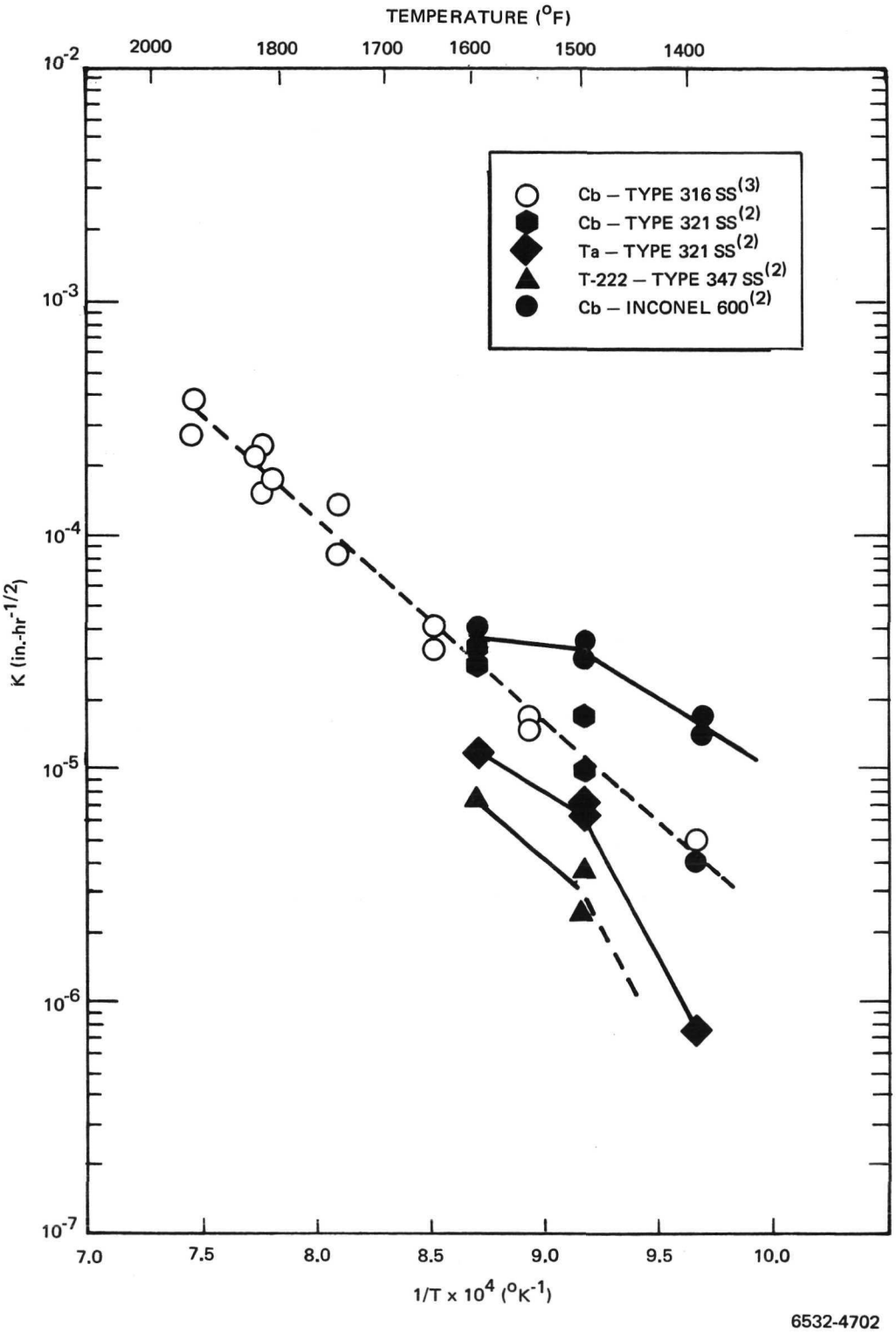

Figure 4. Temperature Dependence of Reaction Rate for Selected Austenitic Refractory Bimetal Combinations

the result of that diffusion on the engineering properties of the bond.[2,3] Both concluded that the properties of the bond began degrading (i.e., the bond region became brittle) after prolonged exposure to high temperatures. While design properties were not developed, it was concluded that the properties had not been degraded significantly, up to the point where the metallographically observed diffusion zone between the two materials was 0.2 mil thick. A diffusion zone 0.5 mil thick, is sufficiently brittle to rupture upon plastic deformation or severe thermal cycling. Figure 4 shows a relationship derived for a number of diffusion couples in the Group Va refractory metals (tantalum and niobium) and conventional iron- and nickel-base alloys. The experiments showed that the diffusion rates of the nickel-base alloys were higher than for the iron-base alloys, the reaction rates were higher with niobium than with tantalum, and an alloy of tantalum (Ta - 8 W - 2 Hf) had a lower reaction rate with austenitic stainless steel than did unalloyed tantalum. One should note that the specific alloy combination for this application was not tested. However, if one were to assume that the diffusion and reaction rate of the Ta - 10 W vs AISI Type 316 stainless steel combination were as great as the niobium vs AISI Type 316 stainless steel combination, then the expected diffusion zone thickness after 40,000 hr at 1250°F would be ~0.2 mil. The reaction would be within the experimentally established limit for a sound joint. If the diffusion rate were lower (closer to the tantalum alloy vs steel system), which is the more likely case, then one would expect that the reaction rate would be reduced by about a factor of 7. Based on the worst case, one would not expect that the diffusion rate would be high enough to adversely affect the engineering properties of the joint during normal operation.

The utilization of the diffusion joint does impose two specific limitations on the system: (1) the combination selected must be fabricable to high-quality standards, and (2) the high-temperature exposures of the joint must be limited to avoid degradation. For example, the diffusion occurring during a 1-hr anneal and solution treatment of the joint would be equivalent to 40,000 hr at 1250°F. The useful lifetime would be "used up" by the heat treatement. This represents one of the quality assessment uncertainties associated with this design approach; at the present time only relatively large diffusion zones

(0.5 mil) can be observed by metallographic procedures. Thus, it is difficult to determine whether some of its useful life has been "used up" by an inadvertent heat treatment. If the reaction has gone to 0.5 mil, the life of the joint has been "used up." Some existing microscopy techniques need developing, specifically for this application, to detect very minute diffusion reactions.

An additional limitation imposed by this joint concept is alloy selection. There has been limited development of transition joints for "gettered" tantalum-base alloys (T-111, T-222, ASTAR 811 C, etc.). Enough work has been done to indicate that the joints can be fabricated (with gettered tantalum alloys); however, a small development program will be required to qualify the joints. Two additional problems can be proposed which may, in the end, restrict the use of refractory metals with hafnium or zirconium additions in this application. The first of these is the potential heat treatment of the alloys, after assembly welding, for enhanced corrosion resistance. The heat-treatment temperature would be ~2300°F in vacuum, and the temperature of the transition joint maintained very low to prevent degradation of the bond. It is not suggested that this cannot be done; but it will not be a simple task. While there is some corrosion-resistance incentive to utilize reactive metal additions which tie up the interstitial oxygen (hence, called gettered alloys), they do impose some additional operation restrictions, and offer additional uncertainties needing resolution. Actual operation of Ta - 10 W to AISI Type 316 stainless steel transition joints in experimental modules indicate that they can be fabricated, integrated into service configuration, and operated in NaK at 1085°F for over 14,000 hr.[1]

B. CORROSION RESISTANCE OF REFRACTORY METAL PIPING

The Ta - 10 W piping in the compact TEM should remain highly resistant to corrosion by the NaK coolant, unless the oxygen content of the refractory metal gets too high.[4, 5] The variation in experimental techniques makes assessment of the level at which the alloy becomes attacked by the coolant difficult to assess; Klueh has observed accelerated corrosion at levels as low as 200 ppm.[5] Until further data come along which refute this, it is considered prudent to assume that, if the oxygen level in the piping in contact with the NaK reaches 200 ppm, then accelerated corrosion can take place. Once the

threshold is reached, one could expect corrosion through the nominal 0.09-in. thick cladding within a relatively short time (days), while operating at 1000 to 1200°F.

Though the corrosion product has not been positively identified, the mechanism proposed is the formation of a ternary or quaternary oxide of sodium, tantalum, and potassium in the base metal. The oxygen is found primarily in grain boundaries and on specific planes in the grains. This accounts for the apparent high corrosion in grain boundaries and along specific metallographic planes, evident in optical microscopy. Corrosion appears at any location in the metal where the oxygen has reached a threshold level.

Samples of Ta - 10 W which have been doped with oxygen and then exposed to NaK or sodium will lose oxygen.[4, 5] The deoxidation is due to two mechanisms: (1) formation of a sodium tantalate, and subsequent solution in the alkali metal, and (2) partition, by solution of the oxygen in solution in the refractory metal into the coolant. The result of the first mechanism is destructive; the oxygen is removed from the structural material, in the form of a corrosion product. The second mechanism might actually provide some protection, during service, by removing the oxygen which can cause corrosion. These are competing mechanisms; and it is difficult, from present data, to determine which one will prevail under any one particular set of conditions.

1. Environmental Contamination

The oxygen can be introduced during fabrication, such as welding or heat treating of the piping in a contaminated atmosphere; or the oxygen content can build up during service, by adsorption of tramp gases in a test chamber. If the gas source is plentiful, and has access to the thermoelectric chamber, one would expect the oxygen level to be significantly higher at the outer surface, and to diminish toward the NaK surface. In this case, once the corrosion began, there would be no mechanism to stop it, other than removal of the pipe from the corrosive media. If the oxygen content of the contaminating environment were low, then one would expect the gradient to be significantly decreased. In this case, some deoxidation mechanisms could be at work during the corrosion.

Three cases of corrosion of Ta - 10 W piping at 1125°F will be considered: (1) operation of a bare Ta - 10 W pipe in 10^{-5} torr oxygen, (2) operation of a module at 10^{-5} torr oxygen, with and without boron nitride covering the piping, and (3) operation of a module at atmospheric pressure, without a complete covering of boron nitride. The cases are typical of proposed or existing ground test environments, and of several presently considered design options. In cases involving operation of a module, it is assumed that there is a very small leak in the stainless steel shroud protecting the piping from the exterior environment. This would be typical of the cases where there were leaks in the power feedthroughs.

If there is no source of oxygen contamination, one would not expect any corrosion to take place; this has been demonstrated by long-term soaking of sealed modules.

In the case of the module operating in air, we assume continuum flow of any gas, and the oxygen incident upon the surface of the refractory metal piping does not form a protective coating. In this case, then, the reaction is not oxygen limited. The time necessary for the oxygen to build up, over the normal 50 ppm of oxygen in the Ta - 10 W piping, would be approximately the quotient of the diffusion rate (5×10^{-9} cm^2/sec) and the square of the piping thickness (0.09 in.).[6] One might expect accelerated corrosion to begin at $\sim 3 \times 10^3$ hr at 1000°F, and at $\sim 2 \times 10^2$ hr at 1200°F. It is reasonable not to expect the calculation to be closer than a factor of 2 or 3 to predicting any specific result.

The failure of Modules TEM-X S/N 3a and 3b after 1200 and 2562 hr of operation at 1125°F is certainly within the range of lifetime which would be predicted by this type of calculation.[1] More precise calculations can be made, but the sensitivity of the phenomena to other variables makes it difficult to predict any more accurately. It appears that the gas leaks observed in the preceding module power pins could be large enough to supply oxygen at a rate sufficient to support the reaction, as predicted from an unlimited source.

As would be predicted by theory, it does not appear that the stainless steel shroud provides any protective barrier for the Ta - 10 W when the oxygen source could be considered as a continuum. However, at very low pressures,

when the oxygen flow would be considered molecular, a different situation exists. The factors governing the reaction kinetics between low-pressure gases and metal surfaces that result in contamination can be deduced from models based on the kinetic theory of gases. The description of the mass flow past any one surface takes a form similar to the Knudsen effusion equation:

$$Q_i = 5.833 \times 10^{-2} P (\mu/T)^{1/2}. \quad \ldots (1)$$

If we consider a bare tube in a vacuum chamber, the mass incident rate, Q_i ($g\text{-}cm^{-2}\text{-}sec^{-1}$), of the gases on a unit area is related to the gas pressure, P(torr), the molecular weight of the gas, μ (g), and the absolute temperature, T (°K). In actual practice, all of the gas molecules striking the tantalum piping are not absorbed by it, giving rise to an experimentally determined parameter, α. This is the probability that an incident molecule will be absorbed by the pipe; hence, it is called the sticking probability. Because of its nature, it is dimensionless. The actual amount of gas that is absorbed by the tantalum alloy piping is related to the product of the sticking probability and the incident rate

$$Q_a = \alpha Q_i. \quad \ldots (2)$$

The pressure in the equation is measured at the chamber wall. Since the pressure in the vacuum chamber is P_o when measured at a temperature of T_o (°K), its pressure at T is greater by the temperature ratio, $(T/T_o)^{1/2}$ $\left[\text{i.e., } P = P_o (T/T_o)^{1/2}\right]$. Substituting this small pressure correction due to thermal transpiration into equation 1 gives

$$Q_a = \alpha\left[5.833 \times 10^{-2} P_o (\mu/T_o)^{1/2}\right]. \quad \ldots (3)$$

To relate this absorption rate to oxygen content, let us further assume that the absorbed gas diffuses into the interior of the metal of surface area $A(cm^2)$ and weight W (gm). The change in concentration, ΔC_m (gm of gas/gm of metal), of the interstitial in the alloy for a reaction time, Δt (sec), is then

$$\Delta C_m = Q_a \Delta t A/W. \quad \ldots (4)$$

Since A/W is equal to A/pV and A/V is equal to 1/X, Equation 4 can also be expressed as

$$\Delta C_m = Q_a \Delta t/\rho X \quad \ldots (5)$$

where:

ρ = density of the piping (gm/cm^3)

V volume of the piping contaminated by the gas (cm^3)

X = thickness of the pipe (cm).

The sticking probability for oxygen and tantalum-base alloys is dependent upon a variety of factors which include, but are not limited to, pressure, contamination level of the substrate compared to solubility of the species, temperature, and surface condition. The factor has not been determined at the temperature of interest; however, it appears to be safe, and not too conservative, to assume that it is 0.2 over the whole range of the application. Table 1 shows the calculated contamination rate, if the diffusion rate of oxygen in tantalum is ignored. Based on the previous cases, it can be shown that, at pressures down to 10^{-7} torr, the factor limiting time to onset of corrosion would be the diffusion rate of oxygen in tantalum. At pressures 10^{-8} torr and below, the limiting parameter is the time required to absorb the necessary oxygen. There is evidence to suggest that the sticking probability is lower than 0.2 at the lower pressures; but it is not strong enough, at this time, to consider altering the calculation.

Table 1 shows that, for long-term operation of a bare tantalum alloy pipe, the pressure should be in the 10^{-9} torr range or less. It also indicates the general operating limits at higher pressures. Note that a delayed failure is predicted by exposure at a high pressure for a short period of time, with subsequent diffusion to the containment surface taking hundreds of hours more.

TABLE I

CALCULATED OXYGEN CONTAMINATION OF 0.09-IN. THICK TANTALUM ALLOY PIPE

Operating Pressure (torr)	Time Required to Reach 200 ppm Oxygen (hr)
10^{-5}	4
10^{-6}	4×10
10^{-7}	4×10^{2}
10^{-8}	4×10^{3}
10^{-9}	4×10^{4}

Assume: Sticking probability, α, = 0.2
As-received oxygen level = 50 ppm
$Q_i = 5.833 \times 10^{-2} P (\mu/T)^{1/2}$
Gas measured is oxygen
T = 300°K

In this case, deoxidation by partition into the coolant could well retard corrosion. The calculations show that the Ta - 10 W pipe could pick up sufficient oxygen in a day of operation at 10^{-5} torr to reach the threshold. The actual corrosion would not be observed for a thousand hours.

The third case considers the operation of a module at 10^{-5} torr, assuming that there will be a leak in the stainless steel outer cladding. For this case, we shall assume that: (1) the leak is equivalent to a square hole, measuring 1 mm on a side (that should be larger than is actually the case), (2) every gas molecule hitting the hole goes through it, and never comes out, (3) all of the gas in the chamber is oxygen or oxygen-producing, and (4) the wall of the test chamber is a significant portion of the test system, and is at room temperature. For the first part of this case, let us also assume that: (5) all the oxygen going into the hole reaches and evenly distributes itself in the Ta - 10 W pipe. [Note that, by actual experience, this is untrue.[1]]

The oxygen flux at the leak can be described by Equation 3. In this case, the probability that the gas striking the hole goes through it is 1 (by

TABLE 2

OXYGEN CONTAMINATION OF TANTALUM ALLOY PIPING IN A LEAKING MODULE

Chamber Pressure P (torr)	Mass Incident Rate Q_i (gm/cm^2-sec)	Mass Accumulation Rate for 1 mm* Q_v (gm/hr)	Contamination Rate for 1 mm, 1 kg* (ppm/hr)	Threshold Time for 1 mm, 1 kg* (hr)
10^{-5}	2×10^{-7}	7×10^{-6}	7×10^{-3}	2×10^{4}
10^{-6}	2×10^{-8}	7×10^{-7}	7×10^{-4}	2×10^{5}
10^{-7}	2×10^{-9}	7×10^{-8}	7×10^{-5}	2×10^{6}
10^{-8}	2×10^{-10}	7×10^{-9}	7×10^{-6}	2×10^{7}

*Assumes leak equivalent to square hole, 1 mm on a side;
Ta - 10 W pipe weighs 1 kg

$Q_i = 5.833 \times 10^{-2} P (\mu/T)^{1/2}$

Gas measured is oxygen

T = 300°K

TABLE 3

TIME TO REACH THRESHOLD CONTAMINATION

Operating Pressure (torr)	Hole 1 mm Square		Hole 0.1 mm Square	
	Case I (hr)	Case II (hr)	Case I (hr)	Case II (hr)
10^{-5}	2×10^{4}	2×10^{3}	2×10^{6}	2×10^{5}
10^{-6}	2×10^{5}	2×10^{4}	2×10^{7}	2×10^{6}
10^{-7}	2×10^{6}	2×10^{5}	2×10^{8}	2×10^{7}
10^{-8}	2×10^{7}	2×10^{6}	2×10^{9}	2×10^{8}

Case I - Oxygen distributed evenly in 1 kg of Ta - 10 W

Case II - Oxygen distributed in 10% of the 1 kg Ta - 10 W pipe

Assume Threshold = 50 ppm as received + 150 ppm = 200 ppm O_2

Gas measured is oxygen

T = 300°K

Assumption 2). The product of the mass incident rate and the area of the hole indicates the mass accumulation rate, or the rate that oxygen is being introduced into the module chamber. If we assume that all of this is evenly divided in the Ta - 10 W, which we shall take to weigh 1 kg, then a contamination rate can be calculated. Table 2 summarizes the calculation for a few cases. It can be seen that the leaking stainless steel cladding restricts access of oxygen to the tantalum alloy piping by a few orders of magnitude, compared with the bare refractory metal case. At pressures in the range of 10^{-6} torr or less, the contamination rate comes to potentially tolerable levels, from a corrosion standpoint. The time required to reach threshold contamination levels is influenced by various controllable factors. Table 3 considers a few of those cases, to show the sensitivity of the lifetime to these factors. A very probable case is one in which the oxygen is concentrated in a relatively small portion of the piping, such as at the ends, where the boron nitride does not cover the refractory metal piping; in that case, the operating pressure would have to be in the 10^{-8} torr range, in order to assure long lifetime. Note, however, that a reduction in the hole size vastly improves the situation; it appears that the lifetime would be adequate, at pressures in the 10^{-6} torr range.

The previous cases considered that all of the oxygen incident upon the holes is absorbed by the Ta - 10 W piping; however, this will not be the case. In present designs of modules to be fabricated, the boron nitride sleeve extends beyond the end of the transition joint, such that the entire refractory metal pipe is now covered. Examination of tested modules indicates that the sleeve is adherently bound onto the piping, offering a good mechanical joint. (1)

If visual appearance is any measure of contamination prevention (at low temperatures, it is not too bad an indication), a boron nitride sleeve prevented discoloration of the Ta - 10 W pipe in at least two modules. (1) If the pipe is surrounded with a high-density boron nitride sleeve, and sealed with good mechanical joints at both ends, then the contamination of the pipe would be further reduced, from the value in Table 3, to that amount of oxygen which could diffuse through the boron nitride sleeve and along the joint at either end. As yet, the diffusion rate of oxygen through boron nitride has not been found in the literature; it is likely that it will not be found, since the diffusion of oxygen through most high-fired refractories at temperatures <1200°F is very low, and

further, boron nitride reacts with oxygen. In all probability, the formation of boric oxide would prevent any diffusion of oxygen through the sleeve, and would tie up the oxygen with stable, nonmobile species, and prevent it from reaching the piping. The remaining case would be the consideration of the diffusion of the oxygen atoms along the mechanical joint.

It is highly probable that the boron nitride sleeve could protect the Ta - 10 W piping from significant contamination over long periods of time at pressures as high as 10^{-5} torr.

2. Internal Contamination

A second source of oxygen for the tantalum alloy piping is the adjacent structural components themselves. The stainless steel piping normally contains a few hundred ppm of oxygen as a normal alloying agent. It acts as a grain and austenite stabilizer. In applications where low-oxygen steel is used, or where it is expected that oxygen will be removed during service, it is common to utilize a vacuum-melted heat of steel. The heat is normally weaker, due to the reduction in the interstitial strengtheners, oxygen and nitrogen; and, in some applications, it may be necessary to provide a special nickel and chrome modification, to prevent the formation of sigma. It is not yet evident that the formation of sigma in this application would be harmful to existing design margins. One could further postulate that any embrittlement accompanying sigma formation could be offset by the decrease in carbon content. In any event, it has been shown that metal atom diffusion across a tantalum - AISI Type 316 stainless steel interface is accompanied, to a great extent, by diffusion of carbon, oxygen, and nitrogen.[2] In accelerated diffusion tests at 1600°F, the steel showed significant losses of the interstitial elements. This was accompanied by grain growth of the affected area of the steel, and an increase in the nitrogen and oxygen content of the tantalum alloy. In one case, the oxygen content was noted to increase from 50 to 110 ppm. Based on this evidence, one can readily postulate that oxygen can diffuse from the stainless steel piping, across the diffusion bond, to the refractory metal piping; and, in time, it can enrich the oxygen content of the tantalum alloy beyond threshold levels for catastrophic corrosion. Deoxidation of the tantalum alloy by the NaK, and diffusion of the oxygen in the structural alloy, however, could prevent the threshold levels from being reached.

Experimental results of actual modules containing NaK as the heat transfer media show that there was no accelerated corrosion of the refractory metal at the bimetal interface. Limited examination and analytical effort is recommended, to establish prevailing mechanisms and verify that oxygen enrichment followed by corrosion will not occur at the transition joint.

3. Summary

Increase of the oxygen content of Ta - 10 W to levels as high as 200 ppm could render the alloy highly susceptible to corrosion by NaK at 1200°F. The oxygen source could come from the operating environment. It could be absorbed by the outer surface, and diffuse into the pipe to the liquid metal surface. For a 0.09-in. thick pipe, calculations indicate that this would take ~3000 hr at 1125°F, if the oxygen source were unlimited. It is calculated that an operating pressure of $\sim 10^{-9}$ torr would be required to prevent contamination of a bare pipe over a long-term application. Calculations show that addition of a stainless steel shroud, even with a leak, decreased the contamination rate when molecular flow conditions exist. Under certain conditions, operating pressures in the 10^{-6} and 10^{-7} torr range would be acceptable, from a corrosion standpoint. The addition of a boron nitride sleeve over the refractory metal piping could well protect the refractory metal piping in an environment where molecular flow exists and there is a finite quantity of oxygen. The boric oxide or the nitrogen formed as reaction products should not adversely affect the refractory metal piping.

A mechanism for accelerated corrosion due to oxygen from the steel piping can be proposed. Tests of actual modules, however, indicate that this does not occur.

C. HYDROGEN EFFECTS

1. Hydrogen in Coolant

The effect of hydrogen upon the mechanical properties of Group Va refractory metals could pose a potential problem on the module piping. Hydrogen is normally found as an impurity in the NaK coolant, as a result of normal permeation out of the fuel element during service. The fuel elements represent a constant source of hydrogen, and diffusion through the reactor piping

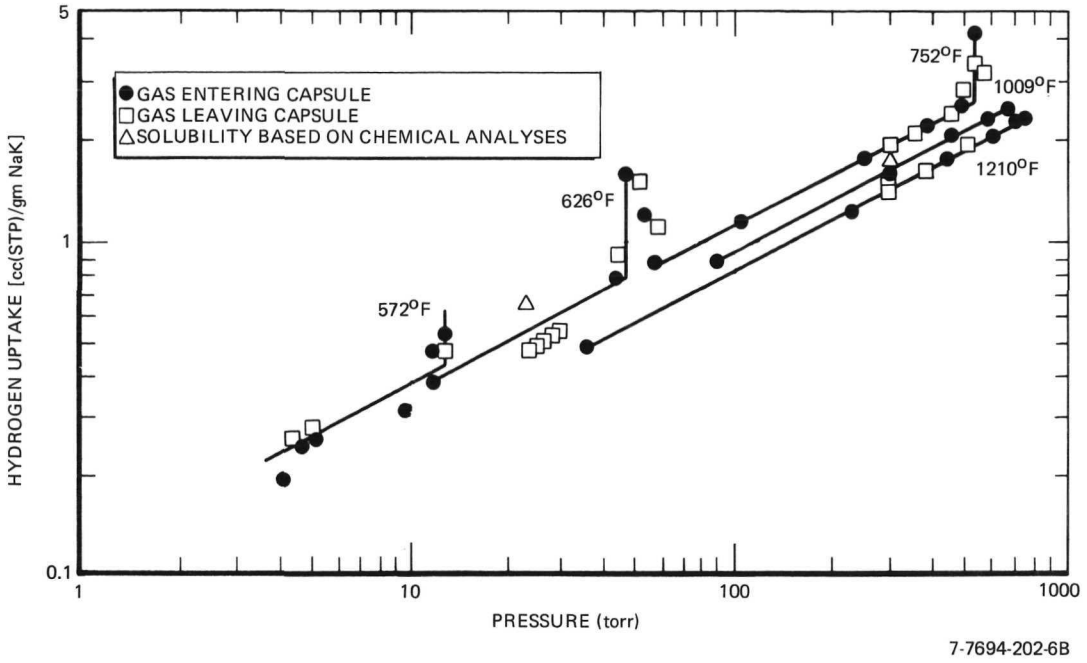

Figure 5. NaK-Hydrogen System[7]

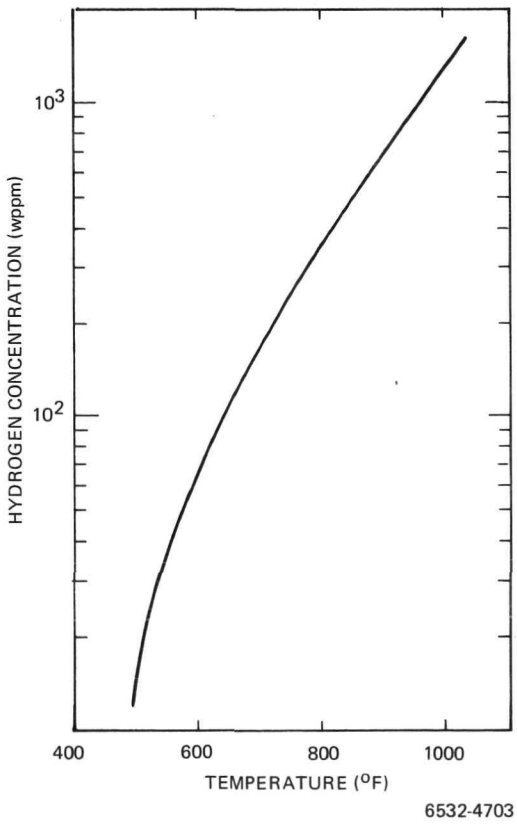

Figure 6. NaK-Hydrogen Solubility[9]

to the environment represents a sink. Under any given set of conditions, the hydrogen content of the NaK will remain relatively constant. This has been calculated to be <5 wppm, for normal operating conditions. Certain accidents or abnormal conditions can be postulated which would increase the hydrogen concentration in the coolant, but it is not expected to exceed 20 wppm. Hydrogen can exist in the NaK in three states, which can be in mutual equilibrium: as a gas, as a solution, and as a compound. Figure 5 shows some of the general characteristics of the hydrogen-NaK system.[7] It can be seen that the NaK will take up more hydrogen as the pressure is increased; and, up to the solubility point, this is not greatly dependent upon temperature. Note, however, that the solubility limit (inflection points in the family of lines) is greatly affected by temperature.

Equilibrium relationships have been developed, over a wide range of pressures. At higher pressures (from ~40 to 760 torr), the relationship takes the form

$$\text{Log } (C/P^{1/2}) = 2.06 + 240/T(°K). \quad \ldots (6)$$

At lower pressures, the equation,

$$\text{Log } (C/P) = 7.765 - 2520/T(°K), \quad \ldots (7)$$

appears to be the proper form.[7, 8] In both equations, C is in wppm of hydrogen in NaK, and P is in atmospheres of hydrogen. The chief differences to be noted between the two are the pressure dependence (square root at high pressures, and linear at low pressures) and the magnitude and sign of the temperature dependence. While the two forms appear to be significantly different, the two relationships are not inconsistent when plotted in their respective regions of high and low pressure.

Figure 6 shows that, at operating concentrations and temperatures, the hydrogen is in solution in the NaK.[9] Above 1000°F, over 1000 wppm hydrogen can be in solution in the coolant. However, on shutdown, the coolant temperature decreases; and, at room temperature, the solubility limit is <5 wppm.

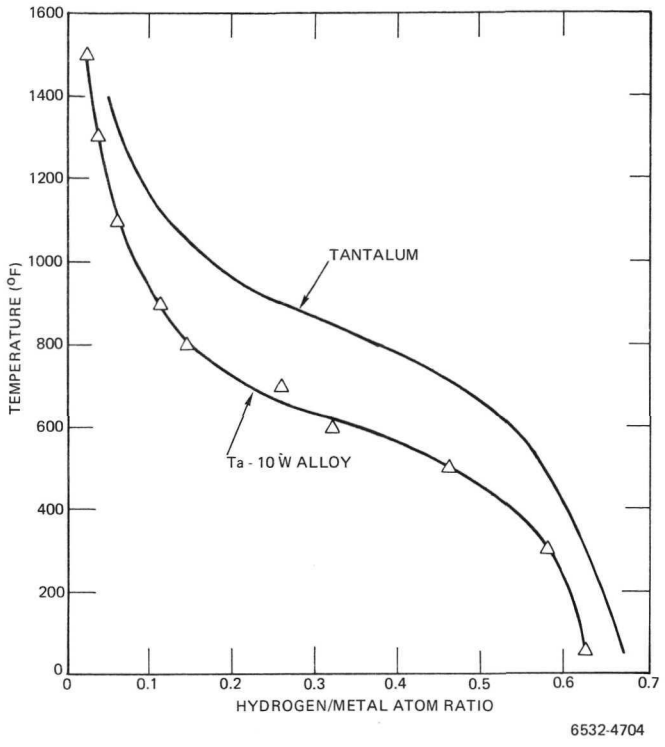

Figure 7. Hydrogen-Tantalum Solubility(10)

Figure 8. Hydrogen-Tantalum Isotherms(10)

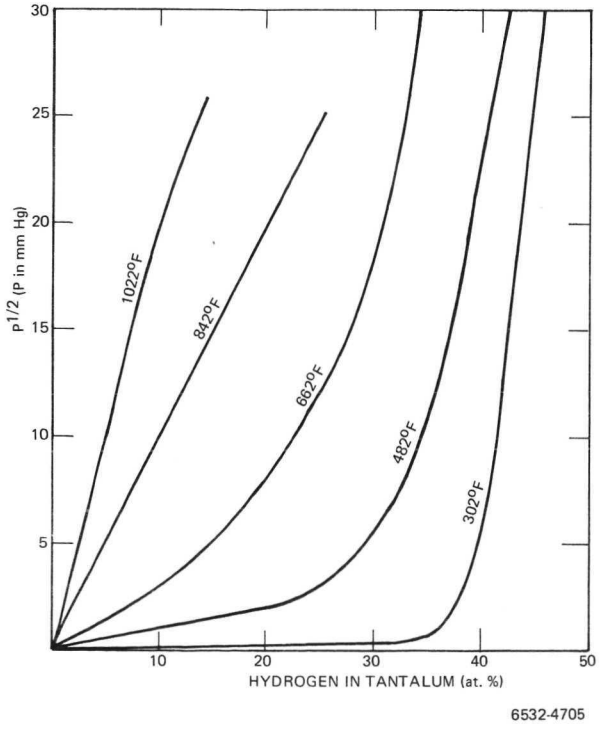

Therefore, at low temperatures, very little hydrogen will be in solution, irrespective of environmental pressure.

2. Hydrogen in Ta - 10 W

In the absence of an external sink for the hydrogen in solution, one would expect the formation of a NaK-hydride during cooldown, as the solubility limit is exceeded. However, if an active sink is provided, one could postulate the transport of some portion of the hydrogen to the sink, the partition of the hydrogen being dependent upon the dynamics and stability of the system components.

Figure 7 presents part of the basis for postulation of this sink.[10] There is a significant solubility of hydrogen in unalloyed tantalum and Ta - 10 W. This solubility increases with decreasing temperature. This is somewhat the opposite of the temperature dependence of the hydrogen solubility in the coolant. Figure 8 shows the temperature and pressure relationship for the capability of unalloyed tantalum to retain hydrogen.[11] While this is not specifically the alloy of interest, experience has shown that the action of the alloy is very similar to that of the unalloyed material, and the relationship can be used as an approximation of the actual case of interest here. Note that, at high temperatures, greater pressures are required for sorption and retention of increasing quantities of hydrogen. More significantly, for any one pressure, tantalum can contain larger quantities of hydrogen at lesser temperatures. At operating temperatures, very little hydrogen is absorbed, even at high pressures. At low, shutdown, temperatures, the alloy can accommodate very large quantities of hydrogen, requiring very little pressure as a driving force. Note that, at 300°F and below, up to 35% of the accommodation appears to be almost independent of pressure.

In contrast to many metals and alloys, it does not appear as though a second phase is formed after some "solubility limit" is achieved. While metal hydrides have been observed in other Group Va metals, such as niobium and vanadium, only alpha tantalum with tungsten and hydrogen in solution has been positively identified in the Ta - 10 W — hydrogen system in the temperature range of interest.

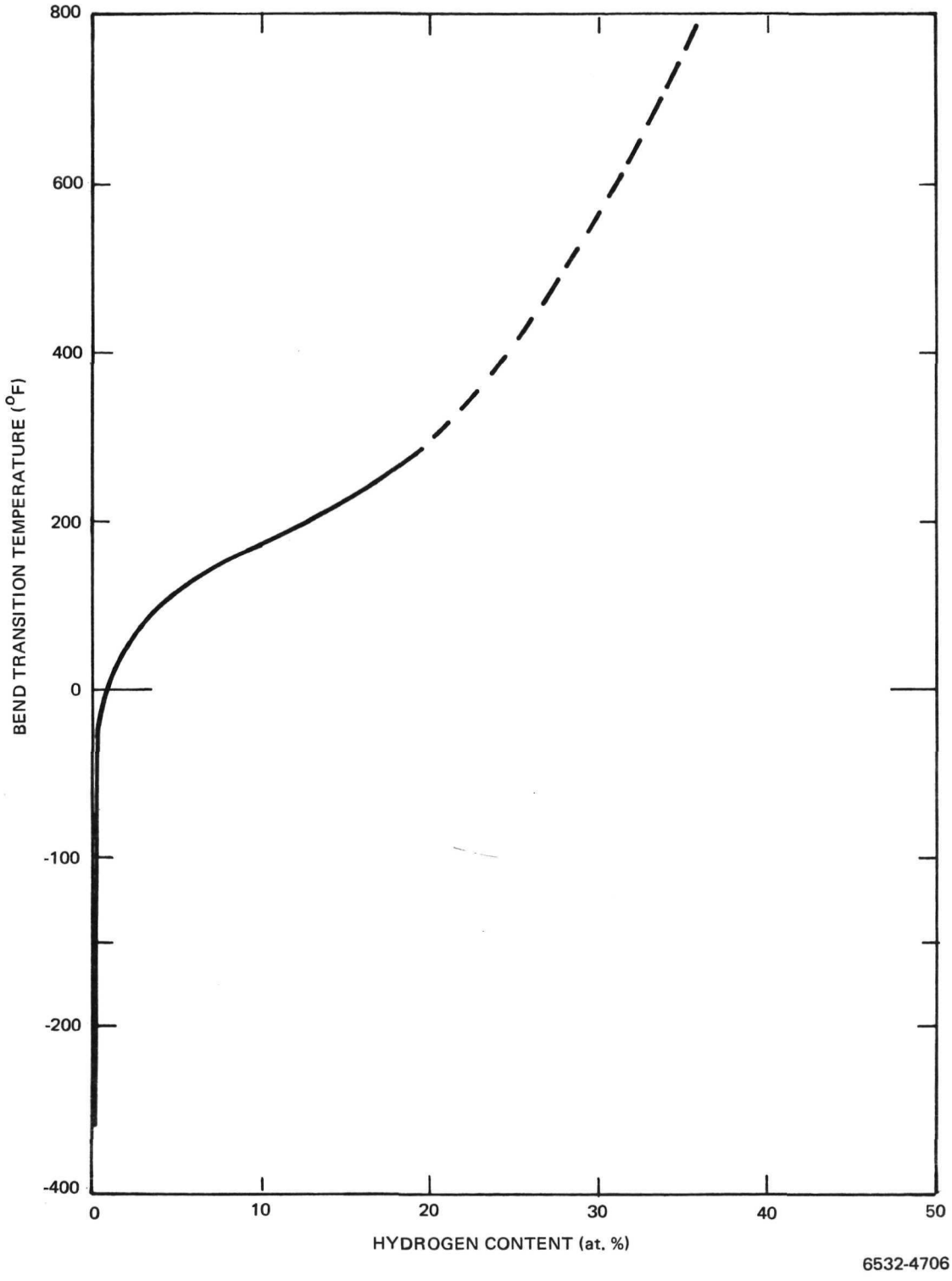

Figure 9. Effect of Hydrogen on Bend Transition Temperature of Ta - 10 W[11]

3. Effect of Hydrogen on Ta - 10 W

Figure 9 indicates what can happen with only very small additions of hydrogen to Ta - 10 W.[12] This is very typical of almost all Group Va metals and alloys. The bend transition temperature is the temperature at which a sheet specimen changes from pass to fail in a bend test. The specimen does not break, when bent about a mandrel with a diameter equal to four times the thickness of the sheet, at temperatures above the transition; the specimen cracks or breaks at temperatures below the transition, for an equivalent hydrogen concentration. While the test is a rather crude one, with pass-fail results, it is a rather inexpensive trend setter. The strain in the outer fiber is calculated to exceed 30% as the specimen is bent past 100°. Those specimens passing the test would most likely represent a ductile condition in a standard tensile test. What is important here is that the bend transition temperature is shifted from nonexistent at liquid nitrogen temperatures in the as-received condition (<5 wppm) to room temperature at 2% (110 wppm). While one cannot say that the alloy is brittle, in the classic sense of the term, the mechanical properties of the alloy have been affected. Even smaller quantities (~16 wppm) have been observed to affect a noticeable change in the engineering elongation in a room-termperature tensile test (from 20 to 5% at rupture).[13]

It is well known that hydrogen can significantly affect the ductility-related properties of all Group Va refractory metals. In fact, hydrogen sorption (sometimes incorrectly called hydriding), deformation, and desorption are probably the primary sources of powdering tantalum and niobium alloy scrap for recycling. Often, mechanical deformation is unnecessary; there is significant strain induced in the metal lattice by the hydrogen in solution. The strain is sufficient, in many cases, for the alloy to fragment spontaneously. This has been observed at levels as low as 28 at. % at room temperature in Ta - 10 W sheet.[13] By referring back to Figure 7, one can see that the alloy will sorb great quantities of hydrogen at 300°F and lower, without much of a hydrogen driving force. Because of this, care is exercised around the alloys, to prevent sufficient impairment of mechanical properties to degrade their use in the system.

4. General Handling Considerations

Given the opportunity, the tantalum alloy piping can and will sorb hydrogen, which can impair its properties. While >28 at. % hydrogen can possibly produce spontaneous fragmentation, only a few percent is required to affect the ductility-measuring properties of the alloy. Figure 7 shows that it is possible for the refractory metal to sorb calamitous quantities of hydrogen at room temperature. The family of curves suggests that tantalum alloys, sitting at room temperature in hydrogen, will destroy themselves; while this has been produced under certain conditions, in actual practice, there is an oxide coating which protects the alloy. The normal self oxidation of the alloy which occurs at room temperature appears to be enough to protect the alloy under most conditions. Industrially, the alloys are heated to temperatures in excess of 1400°F to remove the oxide coating by diffusion into the bulk metal. Following an ~1-hr soak at temperature, hydrogen is introduced, and the charge cooled to room temperature in the hydrogen atmosphere. The retort is opened, any free-standing section is tapped to powder, the retort is resealed, returned to temperature, and evacuated. By referring to Figure 7, one can see that little hydrogen is sorbed at the high temperature; in fact, major pressures (atmospheres) would be required to hold appreciable levels (>5 or 10 at. %) of hydrogen in the tantalum alloy above 1000°F.

While industrial scrap-producing applications utilize removal of the oxide film in their processes to provide uniform sorption of hydrogen, we do know that hydrogen can, in time, diffuse through the naturally occurring film. This, and the difficulty in reproducing various laboratory situations, is believed to be the reason why different room-temperature hydrogen sorption results are achieved in different laboratories or under different operating conditions. This is probably why some test sites have had calamitous results from the cleaning of piping, and others have not.

It is quite likely that a length of Ta - 10 W piping can be cleaned, exposed to normal industrial air, and then to hydrogen, without any degradation of its properties or compromise in its quality. However, if the oxide film were removed from the surface of the piping, the alloy could absorb hydrogen locally. It appears as though, once the alloy begins to sorb hydrogen, it will continue to do so. Spontaneous fragmentation of a Ta - 10 W sheet tensile

specimen began within 20 min after being scratched by a file while in a hydrogen environment, and continued until more than half was in pieces.[13] Thus, exposure of the piping to hydrogen, under conditions where the coating might be removed, should be prohibited. Another example occurred where hydrogen was introduced to an area where a thermocouple had been spot welded to the specimen. Fragmentation began with 1/2 hr of exposure to hydrogen at room temperature.[13] It is not unlikely that the spot-welded area represented an area certainly "cleaned" by the welding, and possibly the oxide coating did not form, as a result of local alloying. This suggests that a transition joint might represent an area of special concern, and should be tested, if it is planned to expose the assembly to hydrogen, even at room temperature.

If an assembly is to be exposed to hydrogen, care should be taken to prevent the tantalum alloy piping from sorbing damaging quantities of hydrogen. Caution should be used in interpretation of parallel prototype tests, for it has been shown that the room-temperature sorption reaction is very sensitive to a number of possibly difficult-to-control factors. One thing which must be avoided is exposure of the piping to hydrogen at a temperature where one might expect hydrogen to diffuse through the coating, or where the coating could be removed, and subsequently cooling the assembly to a point where large quantities of hydrogen will be absorbed. The minimum temperature where the latter might occur is difficult to assess, but could well be 400° F. This should not prevent cleaning components in hydrogen at temperatures above which the refractory metal will sorb large quantities of hydrogen, and then removing the hydrogen by evacuation (for instance) prior to cooling to lower temperatures. Note, from Figure 9, that it requires greater quantities of hydrogen to affect the properties of tantalum at higher temperatures.

While care can be exercised when the assembly will be exposed to obvious hydrogen environments, it is likely that the greatest problems will occur in unexpected hydrogen exposures. An obvious example of this is during cleaning of the alkali metal from the piping. The most commonly used procedures react the coolant with either a hydrocarbon, steam, or water. These are exothermic, hydrogen-producing reactions, known to be violent. Three things all work against the protection of Ta - 10 W. The violent reaction does remove deposits which would be expected to be hydrogen barriers. The heat

produced during the reaction heats up the surface of the piping, increasing diffusion and reaction rates. The hydrogen produced in the reaction is directly available for sorption by the piping. A graphic example of this phenomena displays a niobium-base alloy loop which had been NaK filled, drained, and cleaned with alcohol. While the temperature of the loop never exceeded that of the room, it was rendered brittle, and broke into a number of pieces. (14)

Alternate methods of cleaning which have been successful include the use of mercury, anhydrous ammonia, and distillation. Samples of tubing have been cleaned with copious quantities of water. This appeared to be successful; while not destructively examined in detail, the piping appeared visually and mechanically sound. Post-NaK exposure cleaning procedures should be checked out and verified experimentally, for there appears to be some inconsistency in the scaling up of laboratory tests to actual assemblies.

5. Operational Considerations

During normal operation, the tantalum-alloy piping will be exposed to hydrogen as an impurity in the coolant. The level of hydrogen is expected to be very low, <5 wppm hydrogen in the NaK. The question arises: "How will the operation of the piping be affected by the presence of the hydrogen?" A search of the literature did not yield any experience where a group Va refractory metal was used in the presence of a liquid metal containing small quantities of hydrogen. A model was then developed, in an effort to assess the effect of the environment on the piping.

The model assumes that the relationships developed for the binary systems, NaK(l)-hydrogen (g) and Ta - 10 W (s) — hydrogen (g), can be directly applied to the system NaK (l) — Ta - 10 W (s) — hydrogen in solution. The model assumed that, if the amount of hydrogen in solution in the NaK can be related to the partial pressure of the hydrogen gas over the NaK, and the hydrogen in solution in the piping can be related to the partial pressure of the gas over the piping, then the partition of hydrogen in a NaK—Ta-10 W system is directly related to the equilibrium partial pressure of hydrogen over either species. Webb's relationship (Equation 7) indicates that 10 wppm of hydrogen at 1200°F is in equilibrium with 7×10^{-2} torr hydrogen. According to Veleckis' approximation (Figure 8), that partial pressure of hydrogen over the piping would result in <1 at. %

hydrogen in the tantalum piping. It is assumed that, at any one set of conditions, the partition of hydrogen can be related to the equilibrium activity of the two binary systems, with hydrogen being the common ingredient. This appears to be a reasonable analytical approach at the upper operating temperature. However, when the temperature of the system is reduced, some uncertainties are introduced. These include formation of hydrides, diffusion through coatings which become barriers, and the possible increased competition for the hydrogen by changes in reaction driving forces. An example of this would be to consider that, during shutdown, Figure 5 shows that the solubility of hydrogen in NaK goes from >1000 wppm to ~0 wppm. At the same time, Figure 7 shows that the capability of the tantalum alloy to sorb great quantities of hydrogen is significantly increased. Further, Figure 8 shows that it is at the low temperature where the alloy can least afford (from a mechanical susceptibility point of view) to sorb the hydrogen. Note that the model neglects the effect of the formation of a NaK-hydrogen compound which forms in binary systems at these lower temperatures. Reaction kinetics calculations are not of much assistance in determining the direction and extent of the expected reaction. The analysis indicates that one should not expect a problem, as a result of a reaction between the hydrogen and the tantalum-alloy piping in the normal, high-temperature operating environment. During the elevated-temperature exposure, there is very little driving force for the tantalum to retain the hydrogen, and hydrogen has a lesser effect on the piping's properties. The uncertainties associated with the repartition of hydrogen during a cooling transient are great enough to make difficult, the prediction of what will happen during shutdown.

6. Experimental Program

In an effort to assess the effect of the operating environment, two tests were planned. The first test was designed to verify the form of the model used in the analysis, and the second was to qualify the operation of a module under nominal and off-nominal operating conditions.

a. Partition Model Verification

(1) Test Design and Procedure

A test was designed to expose NaK, Ta - 10 W, and hydrogen in a cell, to observe the redistribution of hydrogen during the cooling thermal transient.

This was the case not clearly defined by the analytical model, and represented potentially the most damaging situation. This was accomplished by sealing NaK and Ta - 10 W samples inside steel ampoules, charging the cell with hydrogen by exposing it to a high-temperature hydrogen atmosphere, and then cooling the three-component system to room temperature for examination. A schematic of the test setup is shown in Figure 10. Specific quantities of hydrogen were charged into each ampoule by controlling the partial pressure of hydrogen in the test chamber. For example, utilizing Webb's relationship (Equation 7) at 1200°F, 3 ppm of hydrogen in NaK is in equilibrium with 3×10^{-2} torr hydrogen over the NaK. In time, the hydrogen in the test retort will diffuse through the ampoule wall, and, when equilibrium is reached, the NaK in the sealed ampoule at the test conditions (3×10^{-2} torr hydrogen at 1200°F) will contain 3 wppm of hydrogen. The partition can be observed by disassembling and examining the three-component system, after cooling to room temperature. The steel capsule, at low temperatures, will prevent the hydrogen from diffusing out of the system. A wide range of impurity levels can be studied in this way. Three test conditions were selected: 3, 30, and 300 wppm hydrogen in NaK at 1200°F. This corresponded to 3×10^{-2}, 3×10^{-1}, and 3 torr of hydrogen as a gas over the NaK.

Following the exposure, the capsules were cooled at 30°F/min, to simulate the temperature change rate of the reactor system. A fourth capsule was exposed, so that NaK containing 300 wppm was cooled at a much slower rate (reaching room temperature in 30 hr), to determine if there were a gross effect of reaction rate. A fifth capsule, identical to the others, was soaked at temperature but in a vacuum, to provide control samples for the experiment. The very wide range and high levels (<5 wppm would be anticipated in a reactor system) were included in the experiment to assure that the very nature of the phenomena were scoped early in the program. Results of the tests would indicate the direction to be taken, if required, in any further evaluation.

The ability of Ta - 10 W to sorb large quantities of hydrogen at room temperature posed some experimental limitations. For example, a small collection of tensile test, chemical analysis, bend test, and archive samples can easily weight ~1 lb. If it is desired to provide sufficient hydrogen in the NaK to allow a reaction to go to completion (e. g., 30% hydrogen in the tantalum

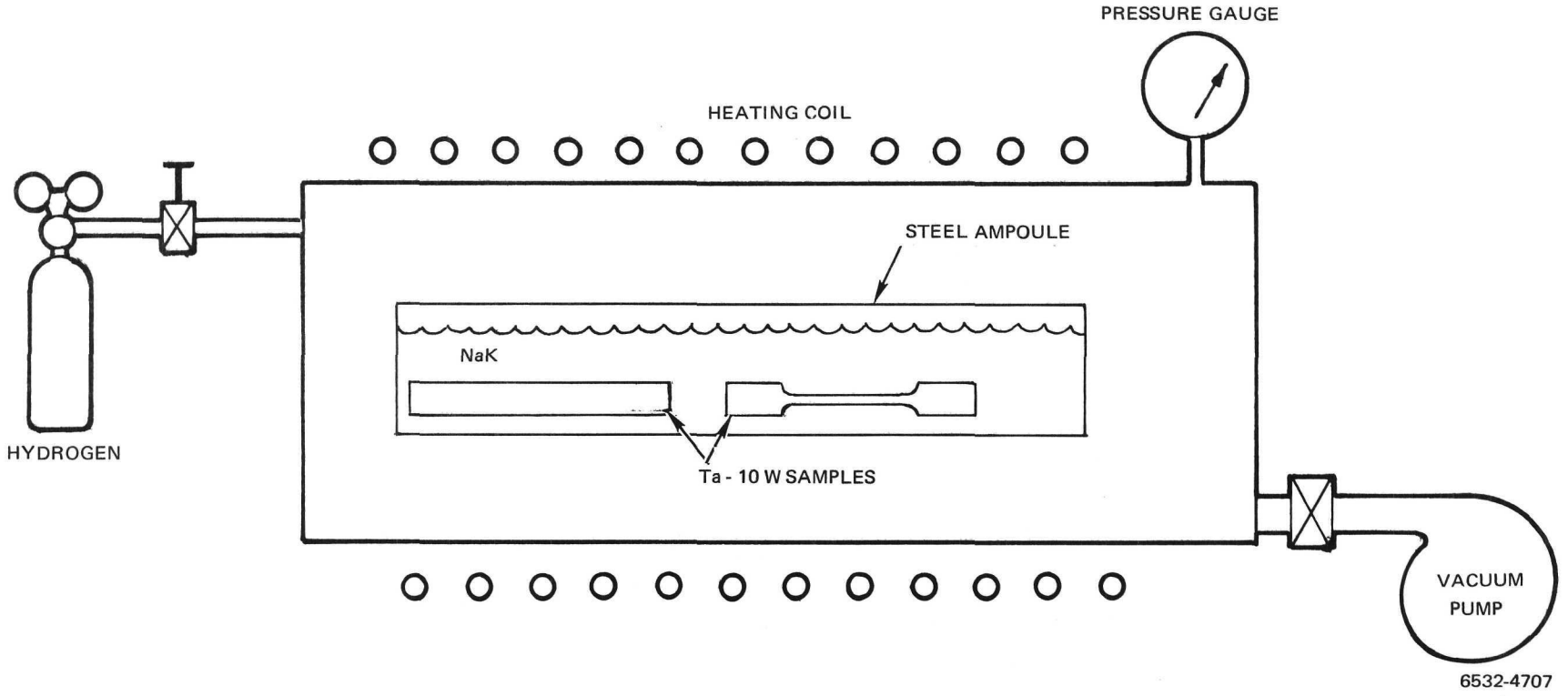

Figure 10. Schematic of Hydrogen Partition Apparatus

alloy), then, for the 3 wppm hydrogen in NaK case, over 250 lb of NaK would be required. Because of this, the experiment was designed to assure that more hydrogen would be available to the refractory metal than in an actual system, but not necessarily keyed to the quantities required for a balanced equation. The approximate proportion of NaK to Ta - 10 W in a reactor system is in the range of 2 (70 lb of NaK to 40 lb of Ta - 10 W). The ratio of ~4:1 (0.85 lb NaK : 0.21 lb Ta - 10 W) was selected as a reasonable balance of specimen and NaK quantity size.

The Ta - 10 W stock used for the test specimens were selected and cut from fully recrystallized tubing, 1.43 in. diameter and 0.03 in. thick. The tubing was produced by spinning to final-size, hydroformed blanks from double electron-beam-melted ingot stock. The grain size of the specimens was ASTM Micrograin Size 6, with a range of half a grain size number. Product chemistry is shown in Table 4.

TABLE 4

COMPOSITION OF HEAT NO. 620024 Ta - 10 W

Impurity Content	wppm*
Niobium	<100
Iron	< 40
Hydrogen	< 1
Nitrogen	15
Nickel	< 20
Molybdenum	< 20
Oxygen	150
Carbon	< 30
Alloy Composition	
Tungsten	10.32%
Tantalum	Balance

*Average of two determinations

Five stainless steel ampoules containing NaK and Ta - 10 W were soaked for over 300 hr at 1200°F in controlled-atmosphere retorts. Hydrogen was bled into each furnace retort to the specified pressures and valved off. As hydrogen diffused through the walls of the ampoules and into solution in the NaK, the pressure in the furnace retorts decreased. It was therefore necessary to adjust the pressure in the retorts during the soaking period, in order to maintain it at a relatively constant level. In time, the hydrogen in the gaseous state outside the capsule came to equilibrium with the gas inside the capsule and in solution in the NaK, and the pressure decrease stopped. It was the diffusion of the hydrogen through the capsule walls which limited the duration of the test. Calculations showed that the 300 wppm case would require ~300 hr for sufficient hydrogen to diffuse through the walls of the ampoule and be in solution in the NaK. The pressure decrease stopped after 260 hr of test, indicating that the system had reached equilibrium. All of the tests were soaked for >300 hr, even though those with lower hydrogen levels were in equilibrium much faster, to eliminate time at test temperature as a test-induced variable.

Following the exposure, the test ampoules were maintained at room temperature (<85°F) until opened in a glove box containing an argon atmosphere. The box gas analyzer indicated <2 wppm each of water vapor and oxygen. One sample from each ampoule was free bent in the box within 20 sec after removal from the NaK, to determine whether the bend transition temperature (BTT) of the alloy had risen to room temperature. The remaining samples from the ampoules were removed from the NaK, and immersed immediately in a pool of mercury. The transfer was immediate (less than a few seconds), and there was no evidence of any warming of the specimens (to redistribute, or otherwise affect, the hydrogen) from the heat of amalgamation, which is fairly large.

The samples remained in the argon atmosphere until it was verified that the cleaning procedure was adequate. A sample of the cleaned Ta - 10 W was removed from the glovebox, and boiled in water for 3 hr. Analysis of the water indicated that <50 μg of residual potassium/cm^2 of specimen was removed. This verified that the specimens were clean.

The specimens were then removed from the box, and the bend tests repeated in a controlled test rig, and room-temperature tensile tests were performed.

Room temperature was selected for both tests, as representative of the most severe hydrogen effect condition proposed for the system. The tensile test specimens were loaded at a rate to produce a controlled strain rate of 0.002 in./in.-min, up to the estimated 0.2% offset load, and thereafter at an estimated 0.2-in./min crosshead displacement.

Interstitial analyses of the samples were performed in three series. They included two separate vacuum analyses for oxygen, nitrogen, and hydrogen [the first by direct vacuum extraction of the gaseous interstitials, the second by fusion of the specimens with platinum - identified (in Table 5) by 1) and 2)], and carbon analysis by combustion in oxygen as the third.

Following tensile testing, samples were microscopically examined by standard optical metallography, and the fracture surfaces by scanning electron microscopy.

TABLE 5

INTERSTITIAL ANALYSIS OF Ta - 10 W
FROM PARTITION VERIFICATION

Identification	Oxygen (wppm)	Nitrogen (wppm)	Carbon (wppm)	Hydrogen (wppm)
As received	1) 10, 40 2) 19, 23	10, 40 2, 6	 24, 16	4, 5 1, 1
Vacuum	1) 28 2) 25, 25	2 10, 12	45, 28	4 10, 11
0.03 torr H_2	1) 11, 67, 18 2) 45, 10	3, 5, 1 20, 14	33, 14	11, 14, 12 12, 4
0.3 torr H_2	1) 13, 50, 62 2) 10, 7	33, 13, 20 5, 7	9, 24	71, 62, 44 4, 5
3 torr H_2	1) 35, 38 2) 40, 35, 4	4, 5 18, 12, 10	36, 23	34, 41 37, 10, 16
3 torr H_2 Slow Cool	1) 2, 35 2) 40, 33	33 10, 9	44, 55	48, 49 35, 35

Ht No. WC 1620024

(2) Results

Results of the evaluation indicated that effects of the exposure could be detected. However, no catastrophic damage was found. The results of the interstitial analyses are shown in Table 5. The overall low levels make for very difficult analysis and wide scatter. However, it is evident that the exposure did not increase the carbon, nitrogen, or oxygen levels. The low oxygen level confirms that the cleaning technique was also very effective. The exposure did increase the hydrogen content of the Ta - 10 W. It would be difficult to separate the vacuum control and the 0.03 torr H_2 groups from each other. There does, however, appear to be an increase (but very small, 5 to 10 over 5) over the as-received level. This indicates that little hydrogen is adsorbed and dissolved at low hydrogen impurity levels (3 ppm H_2 in HaK). There is a significant, though not large, increase in hydrogen content of the samples exposed to the high hydrogen levels. The cooling rate appeared to have little effect on the hydrogen levels of these specimens. Both were about the same (35 to 50 ppm). The scatter in the analysis of the specimens exposed to intermediate levels, and the close proximity of the overall results, makes it difficult to separate these samples from either of the two groups.

Based on these results, one would not expect levels as high as 2 at. % (110 wppm) as a result of normal exposure to hydrogen levels well in excess of the range expected in the coolant. Stephens and Garlick noted a shift of the BTT from "unfound" at liquid nitrogen temperatures to room temperature by the addition of 2 at. % hydrogen.[12] Walter has observed a change in the room-temperature strain at rupture with lesser amounts (16 wppm).[13] It does appear as though some hydrogen will be distributed between the coolant and the Ta - 10 W. While there is scatter in the analysis, there does not appear to be a great increase in the hydrogen sorbed, even at hydrogen levels in the coolant greatly exceeding that postulated for the system.

Table 6 presents the results of the bend tests of the Ta - 10 W sheet. Visual examination of the bend samples indicated a surface roughening on the tension surface on all specimens exposed to NaK. This did not appear to be abnormal, possibly typical of other heats of material, except the as-received sample did not exhibit it. It appears as though the BTT shifted to room temperature as a result of exposure to the NaK calculated to contain 30 wppm of hydrogen.

TABLE 6

Ta - 10 W BEND TEST RESULTS AT ROOM TEMPERATURE

Identification	Free Bend Bend Angle (°)	4t Bend Bend Angle (°)	Remarks
As-Received	150	105	No Cracking
Vacuum	150	105	No Cracking
0.03 torr H_2*	150	105	No Cracking
0.3 torr H_2*	150	105	Surface Cracking
3 torr H_2	90	90	Specimen Broke
3 torr H_2*	70	75	Specimen Broke

*Calculated hydrogen equilibrium

Pressure over NaK (torr)	Impurity in NaK (wppm)
0.03	3
0.3	30
3	300

The transition temperature for the specimens exposed to higher levels is somewhat higher than room temperature. While the specimens exhibited a loss of ductility, one would not consider their behavior to be brittle. It is likely then that an increase of 30 or 35 wppm hydrogen in the Ta - 10 W shifted the BTT from not observed at -325°F (a quality requirement of the raw stock) to room temperature in this heat of material. This appears to be a little more sensitive than that observed by Stephens and Garlick, though not inconsistent with the results of Walter. Note that, even at exposure levels significantly greater than proposed for the system, the alloy retained significant ductility.

Table 7 presents the results of a more controlled test intended to be more discriminating than the bend test. The tensile results indicate that there was no effect on the strength properties of the alloy, as a result of the exposure. Figure 11 shows the very sharp demarcation from elastic to plastic region, marking the 0.2% offset strength typical for the alloy. There appeared to be no

TABLE 7

ROOM–TEMPERATURE TENSILE PROPERTIES OF Ta - 10 W

Identification	Ultimate Strength (lb/in.^{2})	0.2% Offset Strength (lb/in.^{2})	Elongation (% in 2 in.)
As received	87,000	79,200	25
	84,200	75,400	31
Vacuum	80,300	60,600	22
	83,700	70,600	20
0.03 torr H_2*	86,300	74,000	20
	85,300	67,200	19
0.3 torr H_2*	84,200	66,200	23
	87,800	70,000	20
3 torr H_2*	82,900	66,300	8
	81,700	74,000	6
3 torr H_2*	77,300	74,000	4
	84,700	71,600	8

*Calculated hydrogen equilibrium

effect on elastic modulus, ultimate strength, or offset strength. This was not unexpected — these properties are not greatly affected by small hydrogen additions. The ductility measuring property does appear to be affected. Elongation was significantly reduced in the samples exposed to very high hydrogen levels. The levels noted, however, cannot be considered brittle. It is curious to note that the bend test detected a change (surface cracking was observed) in properties in the sample exposed to 0.3 torr of hydrogen. This test did not detect an effect until higher levels. These results confirm that the alloy retains measurable ductility, even after exposure to significantly higher levels of hydrogen than expected in the system.

The surfaces of the tensile test specimens were examined in detail with a scanning electron microscope. The examination confirmed other observations, and served to tie some of the phenomena together. Figure 12 shows the tensile test specimens. Initially, they were all the same length; an untested sample is included in the figure for comparison. Note that the overall lengths of the

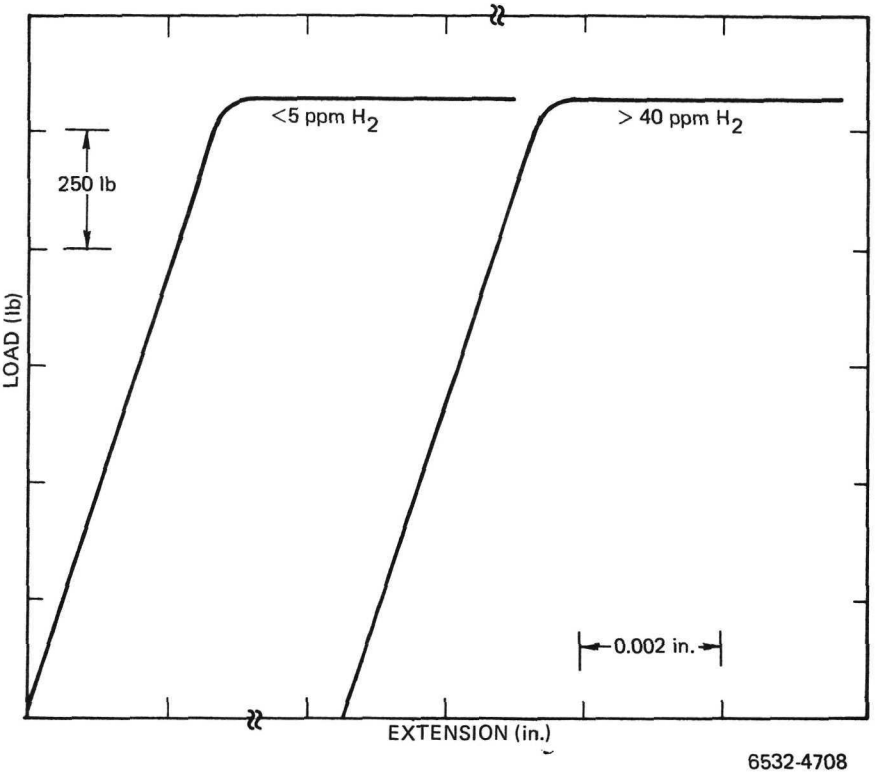

Figure 11. Comparison of Elastic Portion of Room-Temperature Tensile Tests of Ta - 10 W with Different Hydrogen Levels

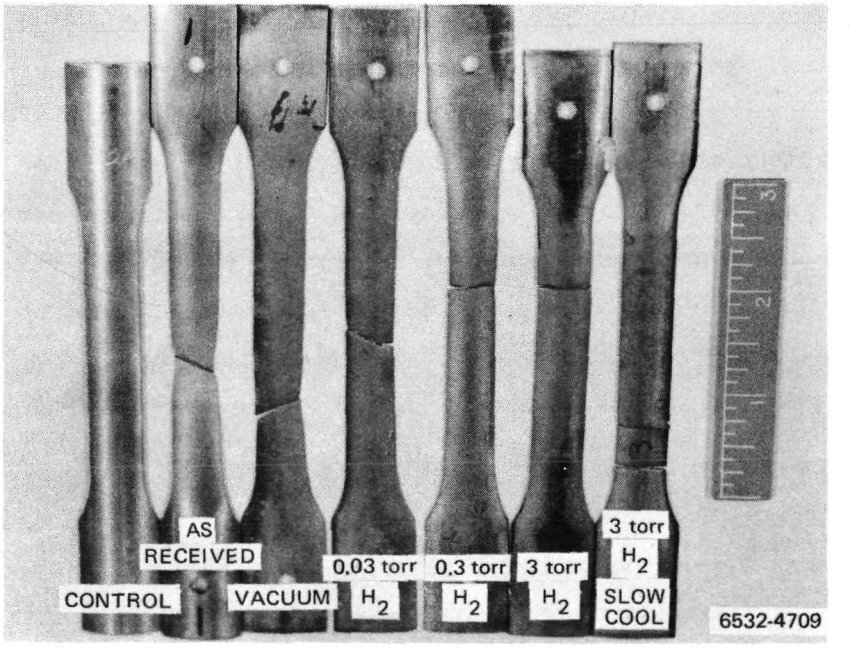

Figure 12. Tensile-Test Samples from Hydrogen Partition Experiment

specimens, up to the pair exposed to the high hydrogen levels, are about the same, providing a visual comparison for the data in Table 7. Note, however, that the angle of fracture, with respect to the tensile load axis, increases with increasing hydrogen content – from 45° in the as-received and vacuum-tested samples, to perpendicular in the high-hydrogen-level samples. The last sample (300 wppm in NaK, slow cool) was damaged during removal of the tensile test extensometer; the double fracture was not an indication of a difference between the fast- and the slow-cooled samples.

Figure 13 shows the intersection of the machined outer surface and the fracture surface, typical of as-received material. The fracture occurred exclusively by ductile rupture. Note also the strain lines on the machined surface of the specimen. They are evidence of high surface strains, and were found only on specimens from this test condition. Figure 14 shows that, with the exception of the original specimen surface, the fracture of the specimen exposed to NaK without hydrogen occurred exclusively by ductile rupture, as in the as-received sample. Figure 15 shows the condition of the original surface of the specimen, for about one or two grain diameters. The brittle cracking occurred all along the specimen surface, where there was strain; it was not observed in undeformed regions outside of the gauge section. The very ductile fracture surface is rimmed with this relatively brittle-appearing region, but it does not appear to have affected the overall rupture strain. The retention of the etched texture on the surface of the specimen indicates that very little strain occurred on the surface of the specimen, prior to the grain boundary separation. This was evident in the bend test specimens, where surface crazing or orange peeling was observed, and, at that time, was not considered uncommon. Detailed examination indicated that the surface texture was not orange peeling, but actual grain separation. Examination of the remainder of the specimens exposed to NaK indicates that this surface condition is present on all of them. It appears fairly uniform, in depth and in general appearance. Figure 15 also shows the appearance of the surface of one of the high hydrogen level specimens. Note that very well-defined grains, indicating little deformation prior to separation, are present. The specimens were etched prior to assembly into the containers, as a normal cleaning procedure. The surface texture of the specimen is

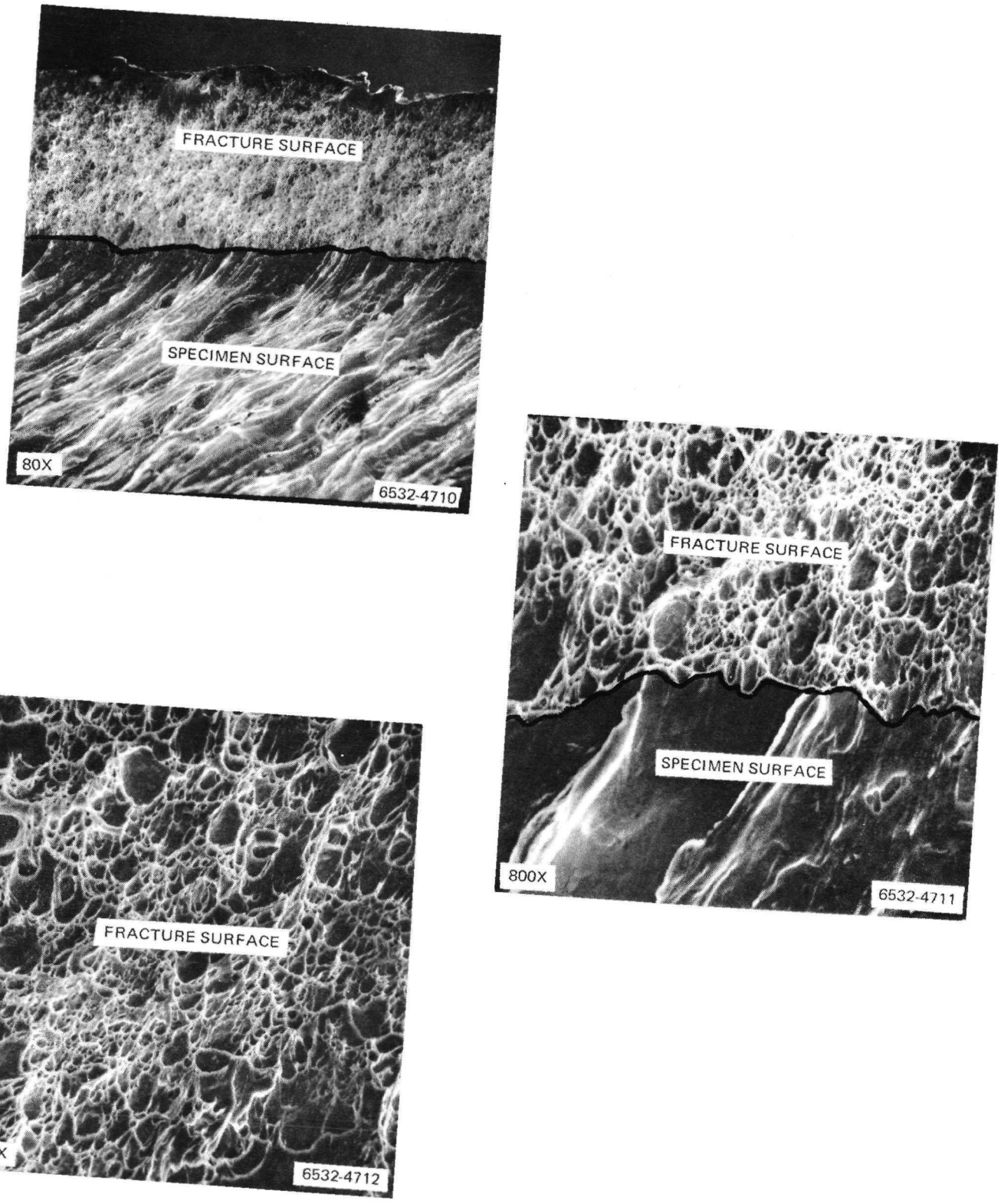

Figure 13. Fracture Condition of As-Received Ta - 10 W

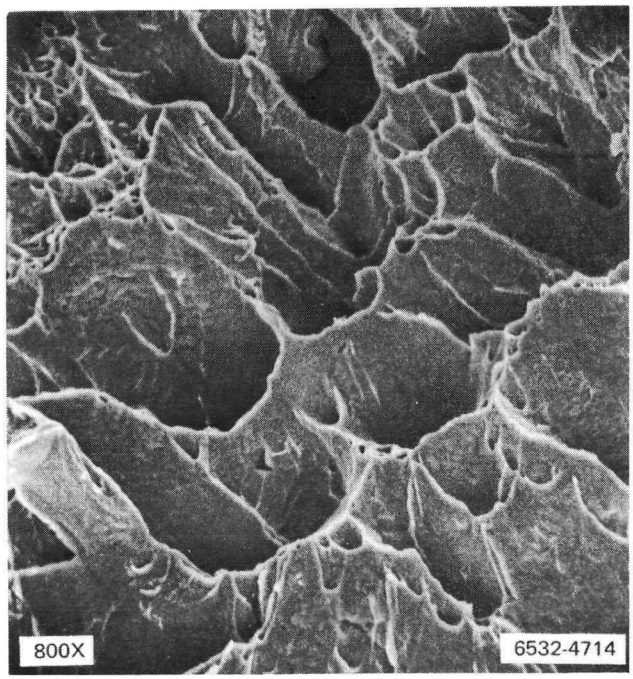

Figure 14. Fracture Condition of Ta - 10 W
Exposed to 1200°F NaK

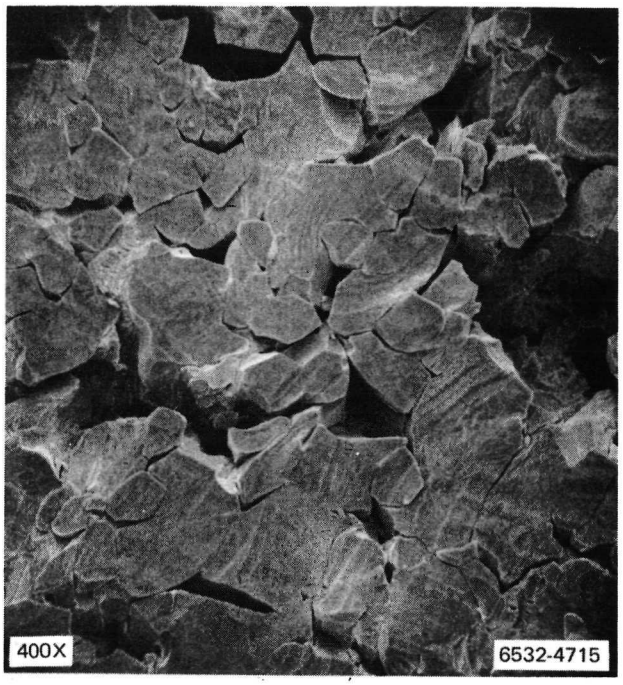

No Hydrogen

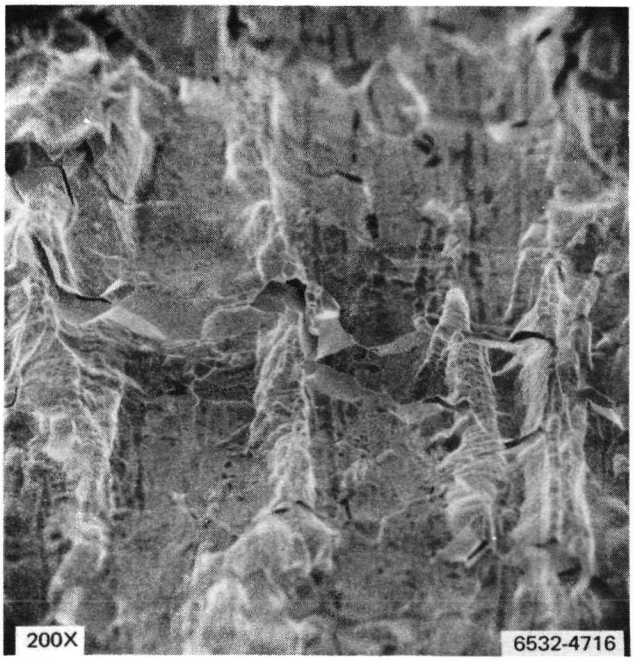

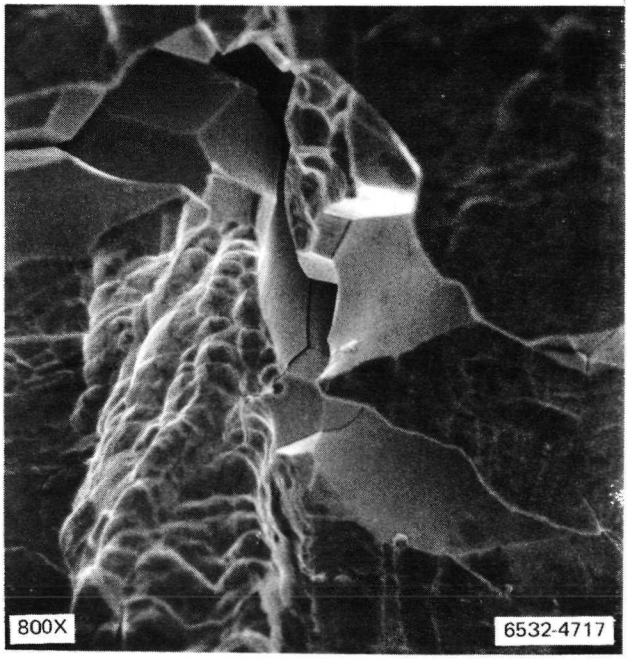

300 wppm Hydrogen in NaK

Figure 15. Typical Strained Surfaces of Ta - 10 W Specimens Exposed to 1200°F NaK

characteristic of a chemically etched metal. The presence of this surface texture establishes that there was no surface removal or deposit, as a result of the exposure.

Figure 16 shows the fracture surface of the specimen exposed to 0.03 torr hydrogen in NaK. This pressure is calculated to be in equilibrium with 3 wppm hydrogen in the NaK. Note that there is a transition taking place. While most of the fracture is ductile rupture, one can detect evidence of grains and boundaries in the rupture surface, indicating a new influence on the rupture mechanism. Note also that there is some evidence of cleavage, though the rupture remains ductile in appearance. The grain boundary separation rimming the fracture surface of all other specimens was also observed.

Figure 17 presents the fracture of the specimens exposed to NaK with 30 wppm of hydrogen. Note that the ductile rupture, evident in the as-received, the NaK without hydrogen, and the NaK with 3 wppm hydrogen specimens, is absent. The whole fracture (save the rim) is cleavage; the surface remains somewhat ductile in character.

Figure 18 shows the fracture of the sample exposed to NaK with 300 wppm of hydrogen. While much of the fracture is cleavage, a significant portion of the fracture has been by grain boundary separation. The figure shows some of the detail of the transition in fracture characteristic. The presence of this failure mode, brittle in nature, does significantly influence the strain at rupture capability of the alloy. It is reduced from $\sim$20% to <10% elongation at failure.

While the examination confirmed the results of earlier tests, it also indicates that some effect was occurring, even at very low hydrogen levels. This effect does not appear to affect the elastic tensile properties.

(3) Impact of Experimental Results

Results of the experiment indicate that the partition of hydrogen between NaK and Ta - 10 W, when cooled from 1200°F to room temperature, will include some sorption of hydrogen by the Ta - 10 W. Within the range studied in this program, which apparently greatly exceeds those levels found in an actual system, the hydrogen sorbed is relatively small. The test confirms predictions that relatively small quantities of hydrogen can affect the properties of the

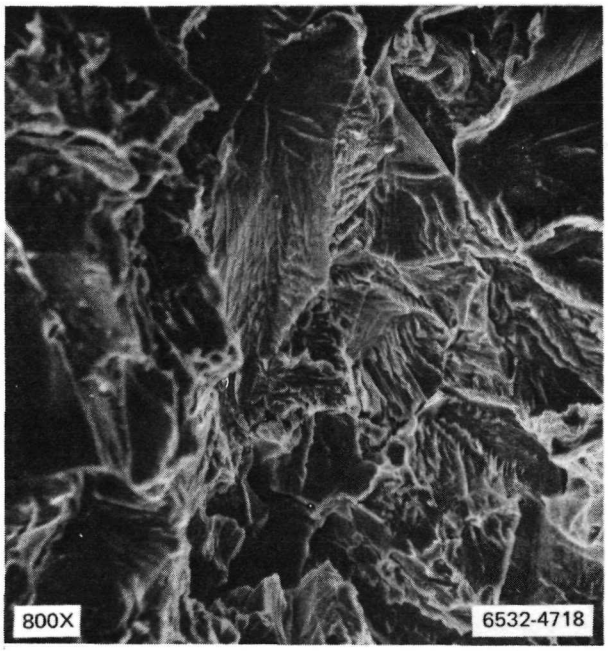

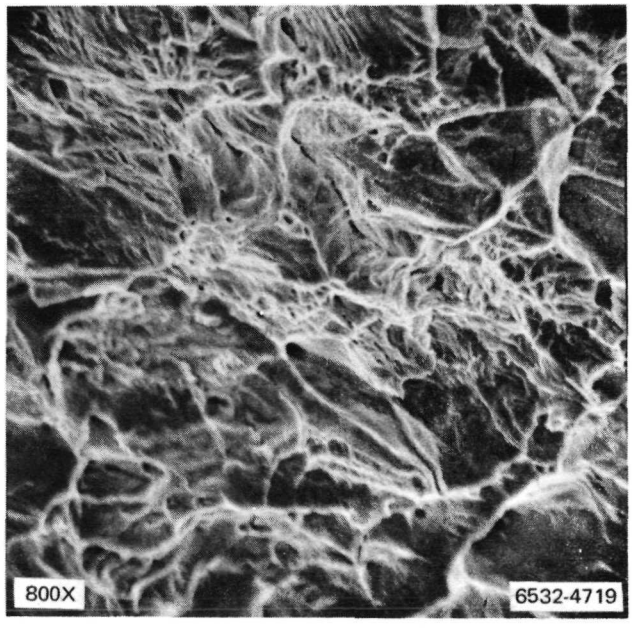

Figure 16. Fracture Condition of Ta - 10 W Exposed to 1200°F NaK Containing 3 wppm Hydrogen

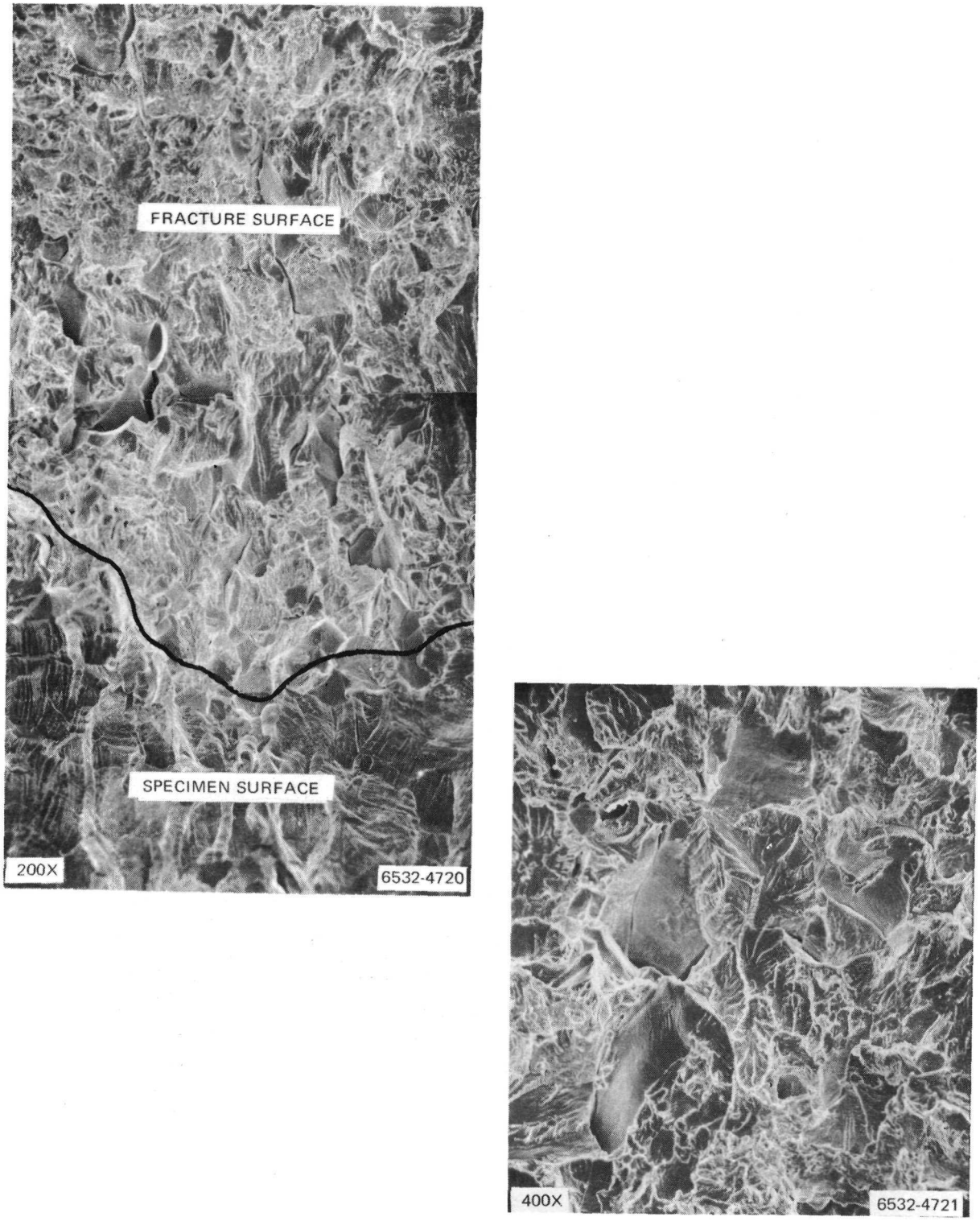

Figure 17. Fracture Condition of Ta - 10 W Exposed to 1200°F NaK Containing 30 wppm Hydrogen

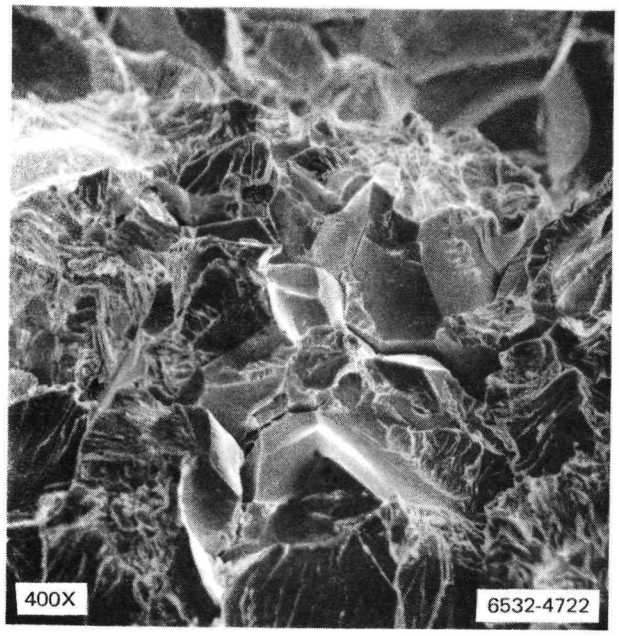

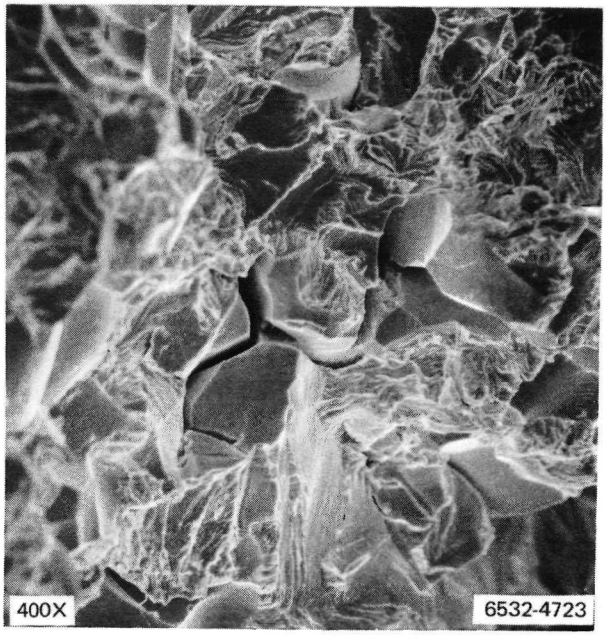

Typical Distribution of Grain Boundary Separation and Cleavage Fracture

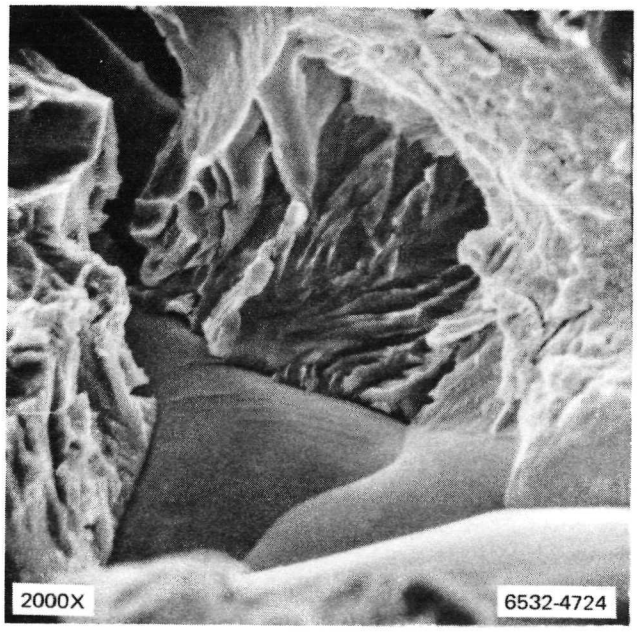

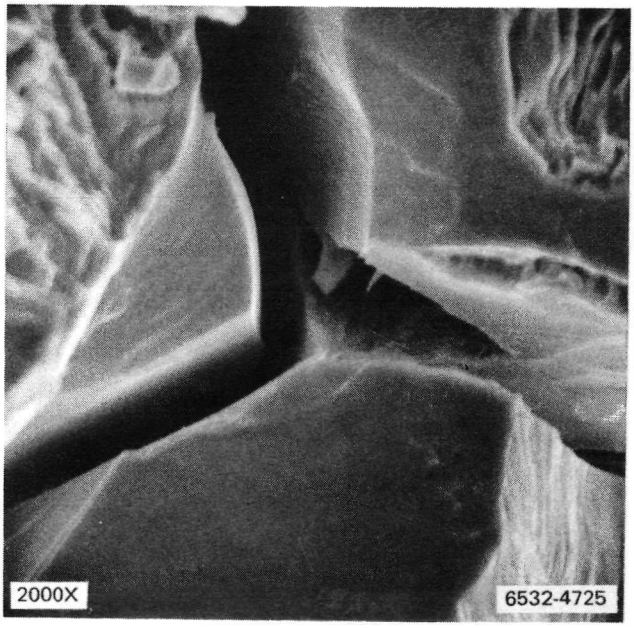

Typical Transition Between Cleavage and Grain Boundary Separation

Figure 18. Fracture Condition of Ta - 10 W Exposed to 1200°F NaK Containing 300 wppm Hydrogen

refractory metal. If we assume that the levels achieved in the experiment do exceed those potentially found in an actual system, then the mechanical properties affected may not affect system design. Certainly, a reduction in elongation at rupture, from 20 to 10%, would not in itself change a design, even 5% elongation will not be required for service. The reduction does indicate a change to the material which probably will affect other properties, such as fatigue or fracture toughness. It is not obvious that these would limit design, either, for there are not a great number of cyclic loads programmed for the system after startup; nor is it anticipated that the piping will contain cracks, as a result of fabrication or service; the relatively thin section also would probably preclude limitation of the system, as a result of classical fracture toughness analysis. The results show that the alloy is affected; while not yet apparent that it will affect design, continued caution is warranted.

b. Module Qualification

Though the partition tests indicated that one should not expect deleterious results as a result of exposure of the Ta - 10 W piping to NaK containing hydrogen, the experiments have serious limitations. These include: (1) having to infer the hydrogen content of the NaK, (2) utilizing stagnant, and not flowing, NaK, (3) using nonprototypic structural shape, and (4) using unloaded specimens during exposure, to name some of the more prominent limitations. Certainly, one would hesitate incorporating a Group Va refractory metal into an actual test system, on the strength of the ampoule tests alone. A more prototypic test was required, and was devised. A NaK loop was fitted with the necessary instrumentation, traps, test sections, and hydrogen membranes, shown schematically in Figure 19. In this loop, an actual module could be operated at various flow rates, temperatures, and hydrogen levels, simulating reactor conditions. In the first series of tests, mechanical and chemical test specimens were encapsulated in the two test sections. The third contained a module inner pipe, clad on the outside to protect it from contamination by air. The system was to be loaded, brought to operating temperature, and the hydrogen level stabilized at 30 wppm (an order of magnitude higher than expected in an actual system).

Following stabilization, one of the test sections was to be valved off, cooled to room temperature, and removed, The specimens were to be removed

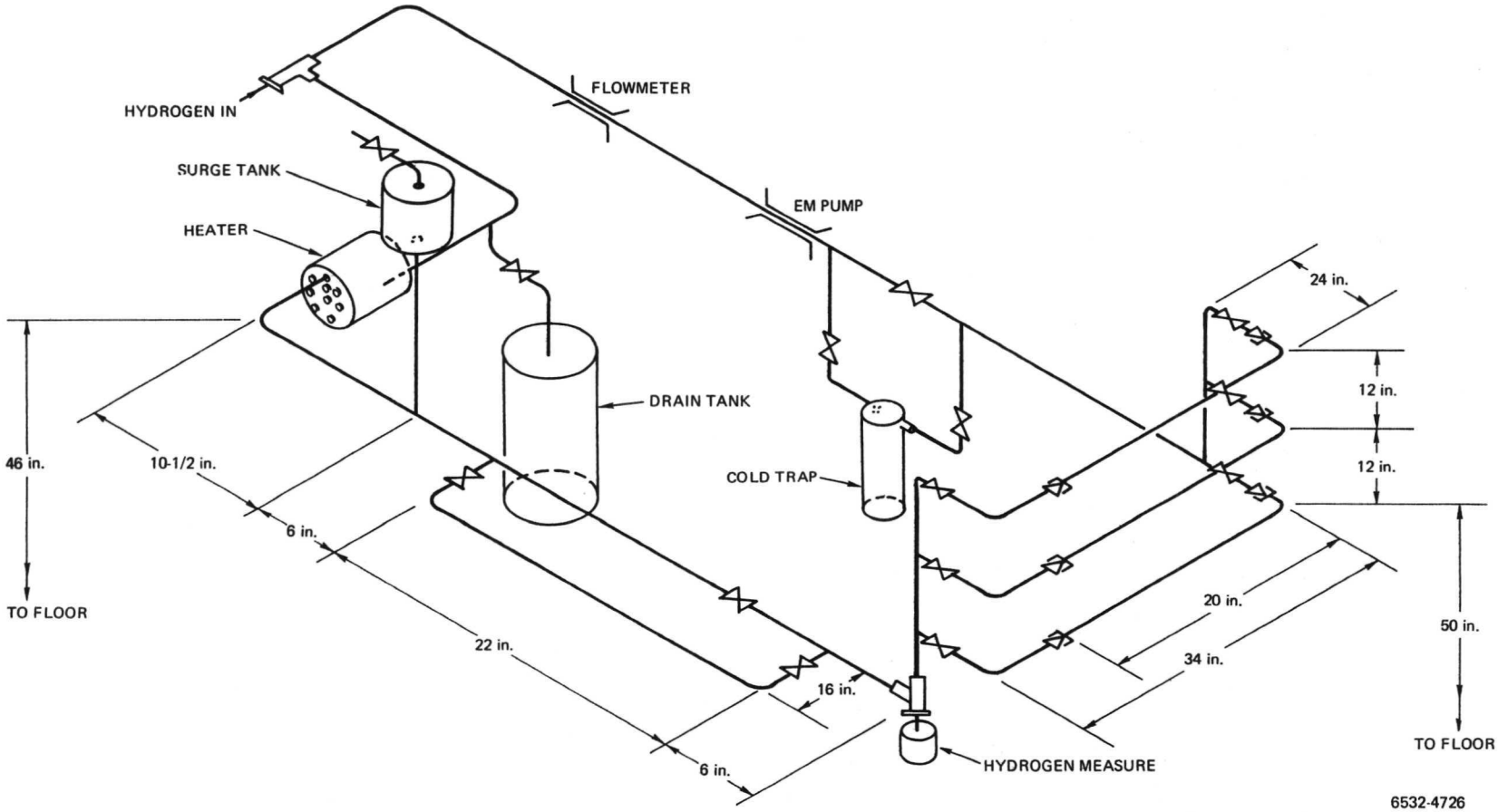

Figure 19. Schematic of Test Loop

from the capsule, cleaned, and tested as in the partition experiments, to determine whether the exposure had any effect on them. Assuming that the results indicated no catastrophic changes to the alloy, the loop then was to be thermal cycled to room temperature 100 times. Following this, the test pipe and sample section were to be cleaned, and tested for evaluation of the effects of the exposure. Assuming that gross, deleterious effects were not observed, an actual module was to be inserted in the test system and exposed to conditions prototypic of, but more severe than, actual operating conditions, as proof that a system can operate in normal and abnormal conditions without breech of system integrity. In the event that the test series indicated potential system difficulties, the severity level of the environment was to be reduced, to retain some margin.

The test loop was modified, the hydrogen analyzer and injector installed, and test sections and test pipe installed. The loop was loaded with NaK, brought up to temperature, and was undergoing intial conditioning when the program was closed out. The loop was drained, and the test specimens removed from the loop and discarded; the inner pipe was drained, cleaned with mercury in air, and stored in air in a wooden box.

7. One Additional Consideration

There is a condition which has not been reviewed, because it is unlikely it could occur in any present system design. It will be included here as a caution, though, in the event an alternate design is proposed where it could occur. Each of the analyses proposed to date assumes that there is either no temperature difference, or at most a small one, between the NaK and the piping; the temperature can range from 1200°F during operation to room temperature at shutdown; there is no provision for part of the system operating at 1200°F and another at room temperature, simultaneously. Plugging of one of the thermoelectric modules would reduce its temperature to approximately that of the secondary loop, ~500 to 600°F. Based on what has been discussed in this report about hydrogen effects and sorption capability, there is little justification to assign any difficulty to this situation. However, if it can be shown that, in a particular design, the tantalum will be at some low temperature (using the bottom curve in Figure 7, let us say, below 300°F) to absorb hydrogen, and the remainder of the system will be at some higher temperature,

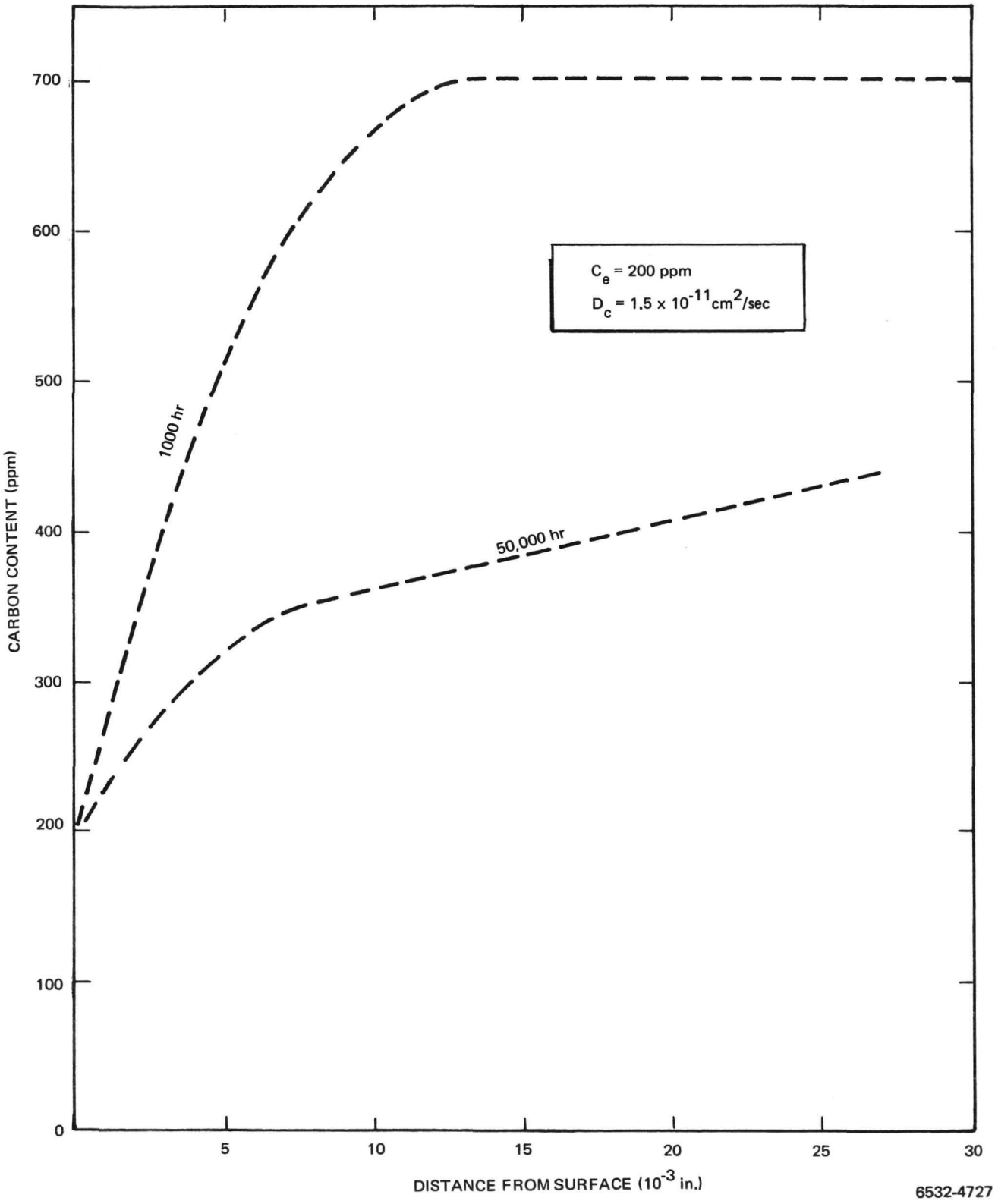

Figure 20. Decarburization of Austenitic Stainless Steel at 1200°F

providing for high hydrogen mobility, then it is expected that hydrogen can and will diffuse through liquid or solid media, down the thermal gradient, and concentrate at the low temperature in the tantalum alloy piping. If this is the case, one can expect potential problems in the system.

D. OTHER INTERSTITIAL TRANSPORT

It has been shown that hydrogen can and will migrate in the reactor system, and, if not carefully controlled, could potentially cause problems. Other interstitial elements (carbon, oxygen, and nitrogen) might also migrate through the coolant system to the refractory metal piping. The elements are soluble in the coolant, and can be removed from a location of higher activity, such as in the stainless steel, to one of lower activity, such as the module refractory metal piping. As a result of this condition, one can postulate a number of results: (1) loss of strength in the steel piping or cladding, (2) loss of austenite stabilizers and formation of sigma phase in the stainless steel, (3) addition of sufficient quantities of interstitials to the refractory metal to embrittle it, or (4) the formation of an adherent "oxycarbonitride" film on the surface of the tantalum, which could decrease the affinity of the piping for the interstitials, to name the more prominent. The nature of the reactions should be evaluated, and the effects on the system operation and reliability assessed.

1. Reaction Kinetics

The migration of carbon, oxygen, and nitrogen from the stainless steel into the coolant and to the tantalum alloy can be readily proposed. Carbon transport in alkali metal systems from one structural alloy to another has been observed for quite some time.[15] However, in this system, the specific operating mechanisms are not well enough known to accurately identify the probable results of long-term exposure. Figure 20 presents the results of an analysis of potential carbon loss from steel piping. The equation was developed as a result of analysis of piping in a NaK loop containing refractory metal specimens.[16] Figure 20 is based on the equation

$$C(x,t) = C_e + \frac{4\left(C_o - C_e\right)}{\pi} \sum_{n=1}^{\infty} \left[\frac{(-1)^{n-1}}{2n-1} \exp\left[-(2n-1)^2\right] \frac{\pi D t}{a^2} \cos \frac{(2n-1)}{a} \pi x \right] . \quad \ldots (8)$$

The analysis shown in Figure 20 assumes that the initial carbon content of the steel was 700 wppm, that the controlling rate is the diffusion of carbon in steel ($D_c = 1.5 \times 10^{-11}$ cm^2/sec), and that there is an unlimited sink for the carbon. It further assumes that the lowest carbon level (C_e) one can expect from the reaction is 200 ppm. D_c and C_e were obtained from decarburization of stainless steels in sodium systems.[15] If one assumes that loss of carbon to <500 wppm would require a strength penalty in design, then it can be seen that, in time, an effect can be noted.

If, however, a layer of Ta_2C or TaC is formed on the surface of the tantalum alloy pipe, then one would expect the diffusion coefficient in the equation to be increased from 10^{-11} cm^2/sec to 10^{-13} (for Ta_2C) or 10^{-14} cm^2/sec (for TaC). If this occurs, one might expect that the transport will stop; and there will be little effect (if any) on the steel, as a result of the introduction of the refractory metal. An experiment was proposed which would attempt to verify the form of the equation used in the analyses, test some of the assumptions, evaluate the applicability of the present empirical constants, and determine the nature of the diffusion and reaction products. Three-component capsules were selected for this experiment. They were AISI Type 316 stainless steel capsules containing NaK and Ta - 10 W mechanical and chemical test specimens.

Four test conditions were proposed: isothermal capsules at 1100, 1200, and 1300°F, to evaluate the isothermal kinetics of the reactions, and a thermal gradient within the capsule, in an effort to determine the various natures of the real-life reaction products. It is not unlikely that different reaction products will occur, as a result of a thermal gradient in the system. The test series was designed to determine this, and qualitatively assess its effect on the analysis. There were three capsules selected for each test condition, for examination after 1000, 3000, and 8000 hr. Twelve capsules were used (three capsules each at four test conditions). The capsules were sealed in

helium-filled quartz ampoules to prevent interaction of air with the reactions taking place inside the steel capsules.

The capsules were fabricated, and the thermal exposure begun, when the program was closed out. There being too little time on test (<500 hr) for fruitful examination, the capsules were discarded.

2. Effect on Mechanical Properties

The net transport of the interstitial elements could well change the properties of the structural members. The loss of interstitials from the austenitic alloys could impair both the long-term creep and elastic properties.[17] Addition of interstitials to the refractory metal would not be expected to affect any diffusion-controlled mechanical property (operating temperature too low); but elastic properties, such as strength or ductility, may be affected. An experiment was proposed where long-term effects on the stainless steel would be observed; and then, at the end of that observation (10,000 hr), the resultant effect on the elastic properties of the tantalum and austenitic alloys could be evaluated. The test utilized the same technique employed by Atkins to observe the strength of steels tested in sodium.[18] Figure 21 shows schematically the test setup for the experiment. Twelve AISI Type 316 stainless steel thin-wall tubes in the annealed condition were installed in the retort. The heat of material had previously been tested by Atkins[18] at 1200°F. The composition of the heat is shown in Table 8. The specimens were individually pressurized with helium to provide the biaxial stress in the NaK-filled retort. Thin-walled tubes were used to increase the rate at which an effect should be observed. The 1200°F test temperature was selected, slightly above operating temperature but still within its regime. Ta - 10 W tubes and strips were placed in close proximity to the specimens, as shown in Figure 22. The twelve specimens provided for three specimens at each of four selected stress levels. The stresses were selected from actual test data on the heat of material, when tested in helium to produce rupture in 1, 3, 5, and 10 x 10^3 hr.

The specimens were installed in the rig, and the test was started and underway for $\sim 3 \times 10^3$ hr when it was shut down at the close out of the reactor development program. Nothing out of the ordinary happened. Specimens ruptured about as expected. Figure 23 and Table 9 show the results of the test,

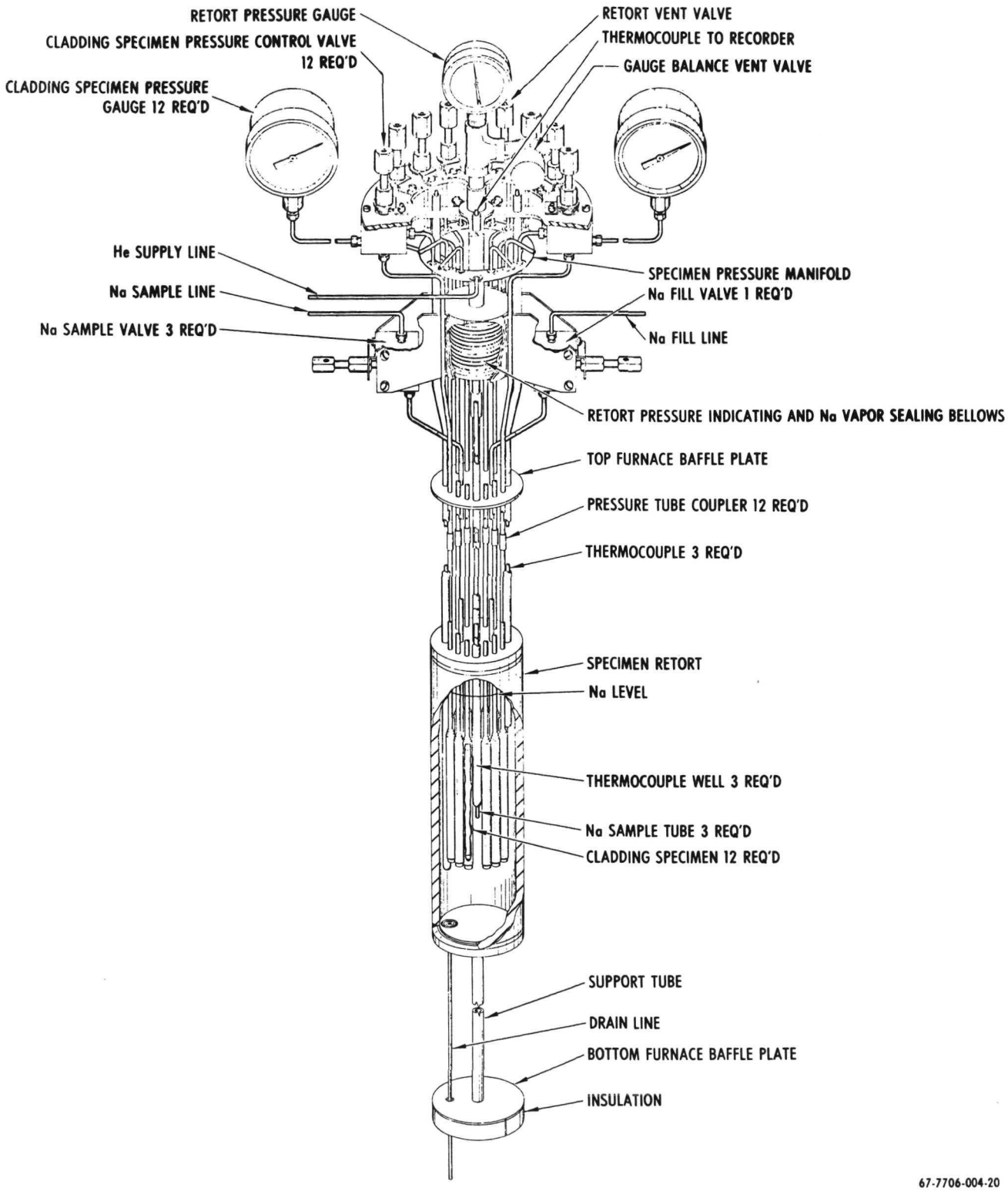

Figure 21. Schematic of Biaxial Stress-Rupture Test Setup

TABLE 8

CHEMICAL COMPOSITION OF AISI TYPE 316 STAINLESS STEEL, HEAT NO. 65808, ANNEALED CONDITION (0.298-in. OD by 0.010-in. Wall)

Element	wt%
C	0.06
Mn	1.82
P	0.004
S	0.002
Si	0.44
Ni	12.49
Cr	17.30
N	0.025
Co	0.041
Cu	0.008
Mo	2.50
B	0.0007
Fe	Balance

compared with the specimens tested without the getter, Ta - 10 W.[18] From the data available to date, it appears as though the exposure had no effect on the properties of the austenitic alloy. There does appear to be an increase with time in the diametral strain at rupture. This increase in ductility would be the direction one might expect with a loss in interstitial strengtheners; however, this appears to be similar to the helium control samples. Analysis of the samples for carbon indicates that there was possibly a decrease of up to 100 wppm (from 650 to 550 wppm). This is too small a decrease to be of significance. Analysis of the tantalum alloy specimens indicates that any change in carbon level is just too small to be detected, above the 25 wppm level of the starting material.

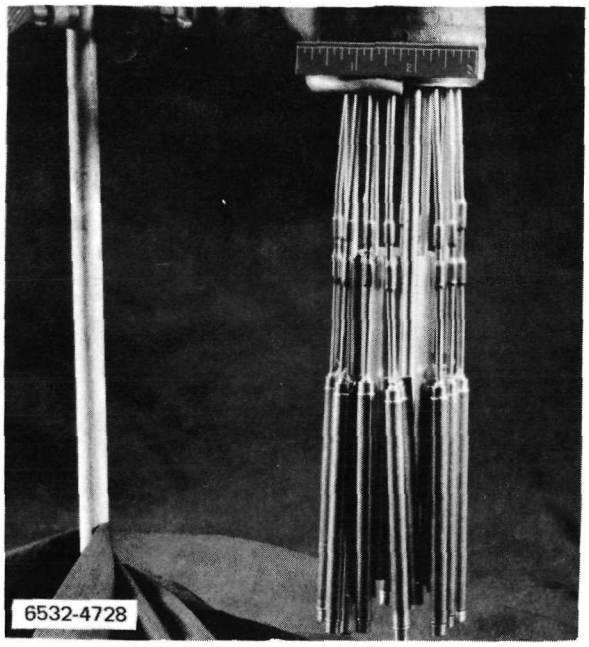

a. Overall View of Test Assembly

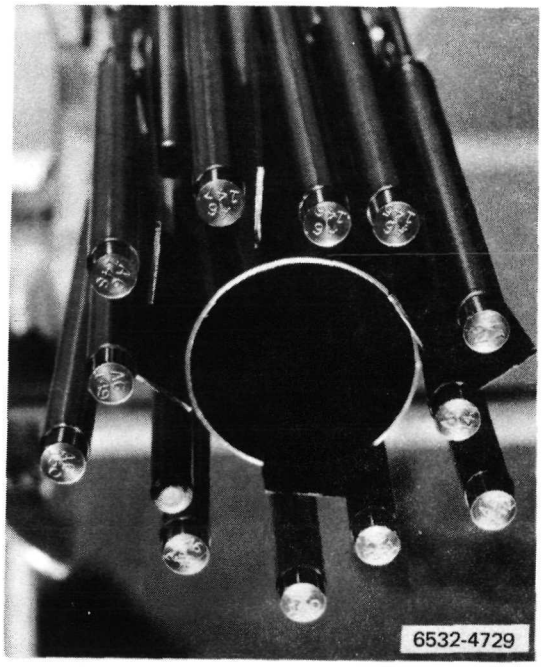

b. Steel Test Specimens and Ta - 10 W Tube and Strips

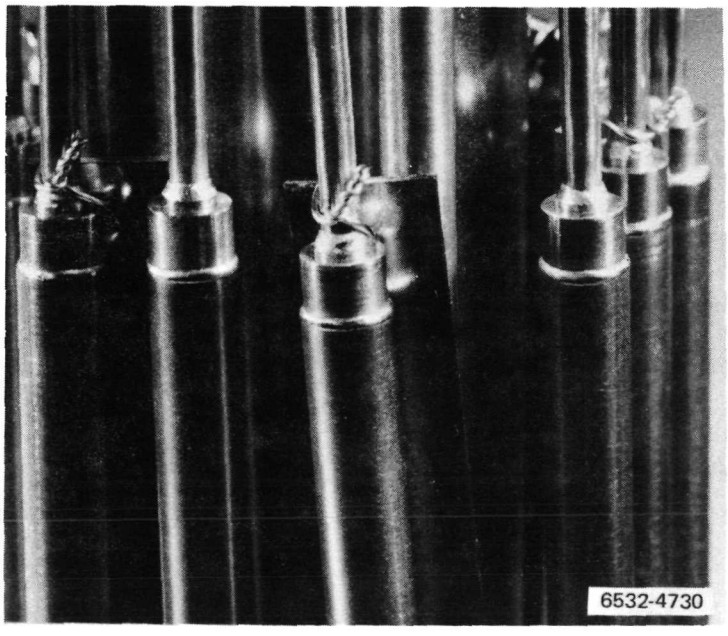

c. Attachment of Strips to Pressurization Tubes

Figure 22. Configuration of Test Specimens

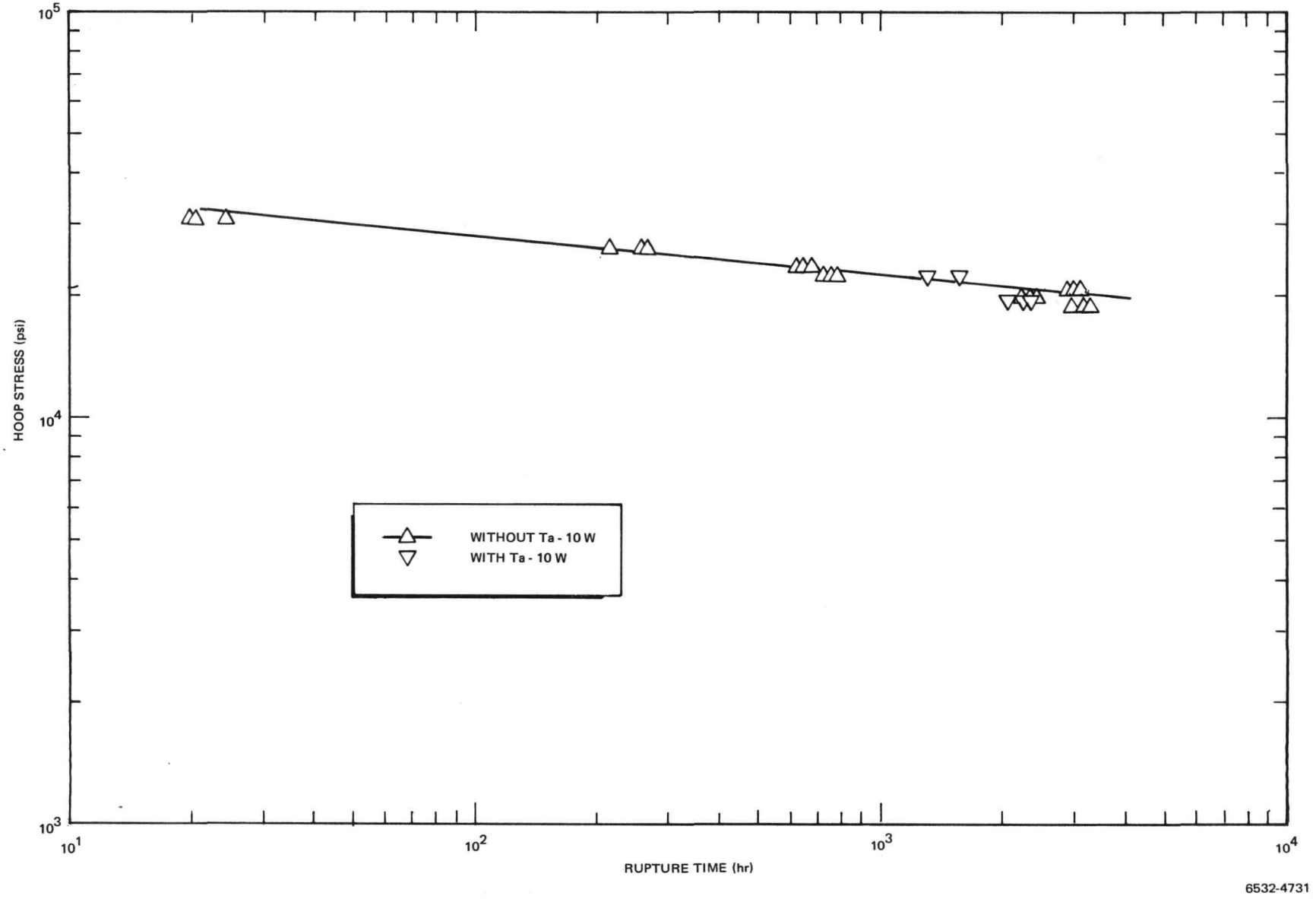

Figure 23. Biaxial Stress-Rupture of AISI Type 316 Stainless Steel in Sodium at 1200°F

TABLE 9

BIAXIAL STRESS-RUPTURE TESTS OF AISI TYPE 316 STAINLESS STEEL, HEAT NO. 65808, 1200°F STATIC SODIUM

Tube Number	Hoop Stress (psi)	Rupture Time (hr)	Diametral Strain (%)
139	22,260	1344	13.0
140	22,260	1572	14.0
142	20,020	2078	22.0
143	20,020	2342	19.0
144	20,020	2246	12-17
145	19,000	3014*	10.5
146	19,000	216*	1.0
147	19,000	3014*	6.5
148	18,000	3014*	1.0
149	18,000	3014*	6.0
150	18,000	3014*	8.0

*Test terminated before rupture.

Rupture in all of the specimens were very small, requiring an over-pressure of a number of atmospheres after test to permeate helium.

Figure 24 shows the structure of the stainless steel prior to exposure at 1200°F to NaK containing samples of Ta - 10 W. The uniform grain size (ASTM micrograin size 5 to 5-1/2), single-phase structure, typical of annealed stainless steel cladding, is evident. The metallographic examination indicates that there was no metallic corrosion or deposition as a result of the exposure, and the carbide precipitation appears to be relatively uniform and not significantly dependent upon stress. However, the very-high-strained regions (~50% local reduction) of the two high-stressed samples do appear to exhibit more precipitates than those at the remaining test conditions. It is more likely due to

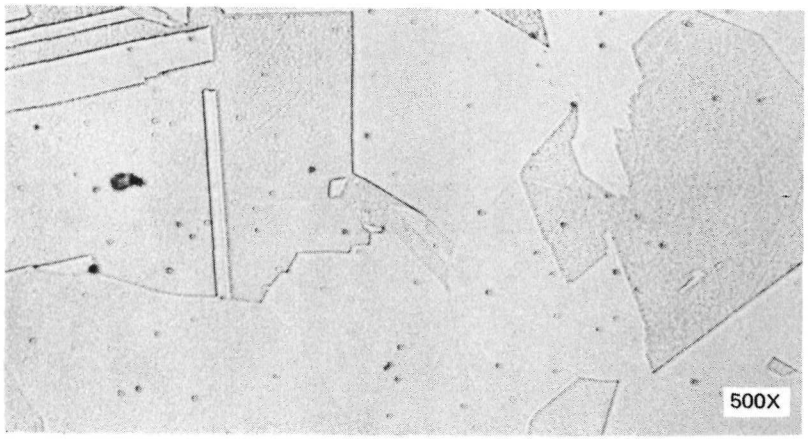

9830-9

a. As Received

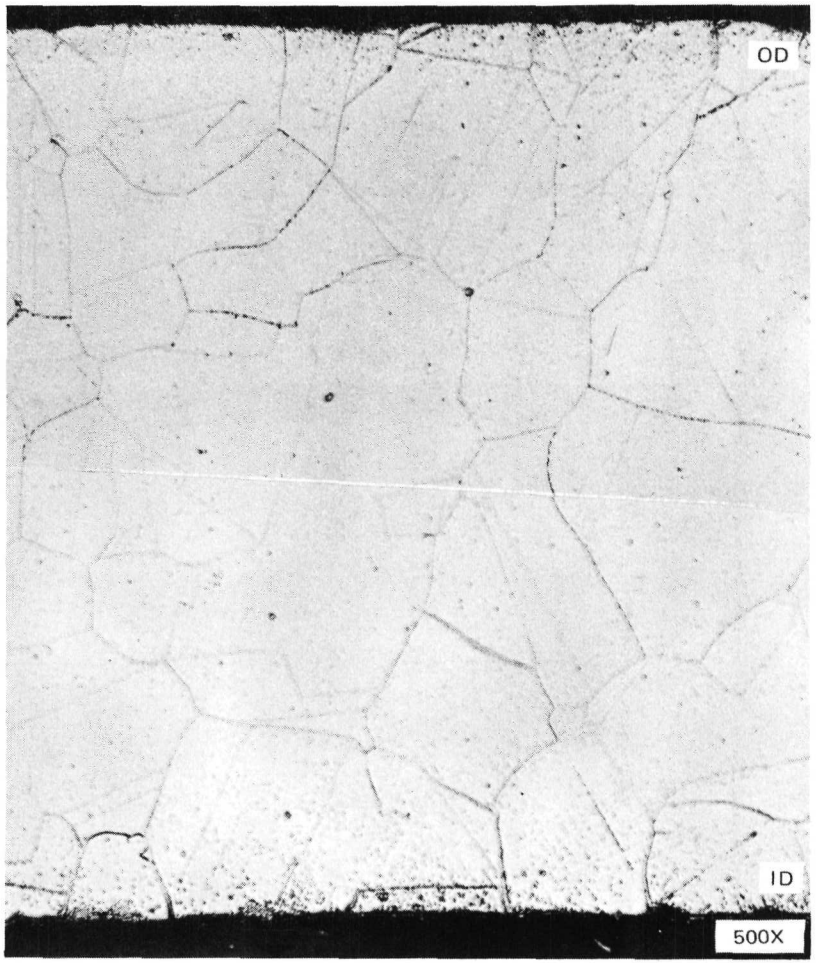

9830-7

b. Exposed to Test Environment Unstressed

Figure 24. Microstructure of AISI Type 316 Stainless Steel Biaxial Stress-Rupture Specimens
(Sheet 1 of 4)

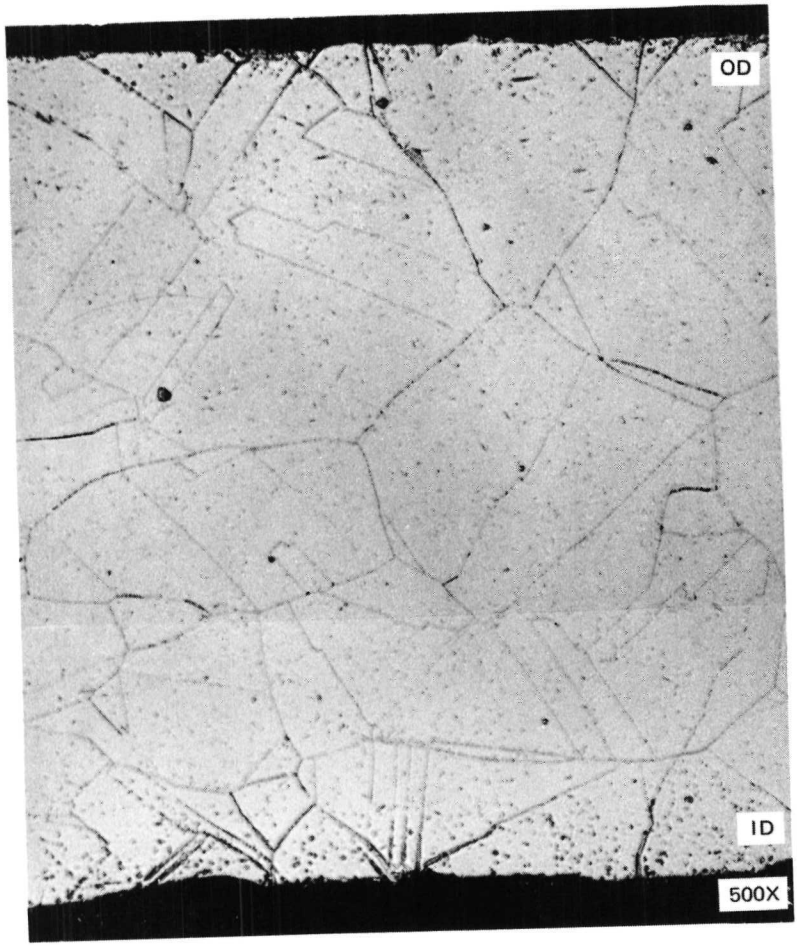

9830-8

c. 18 ksi Hoop Stress, 8% Diametral Strain, Not Ruptured

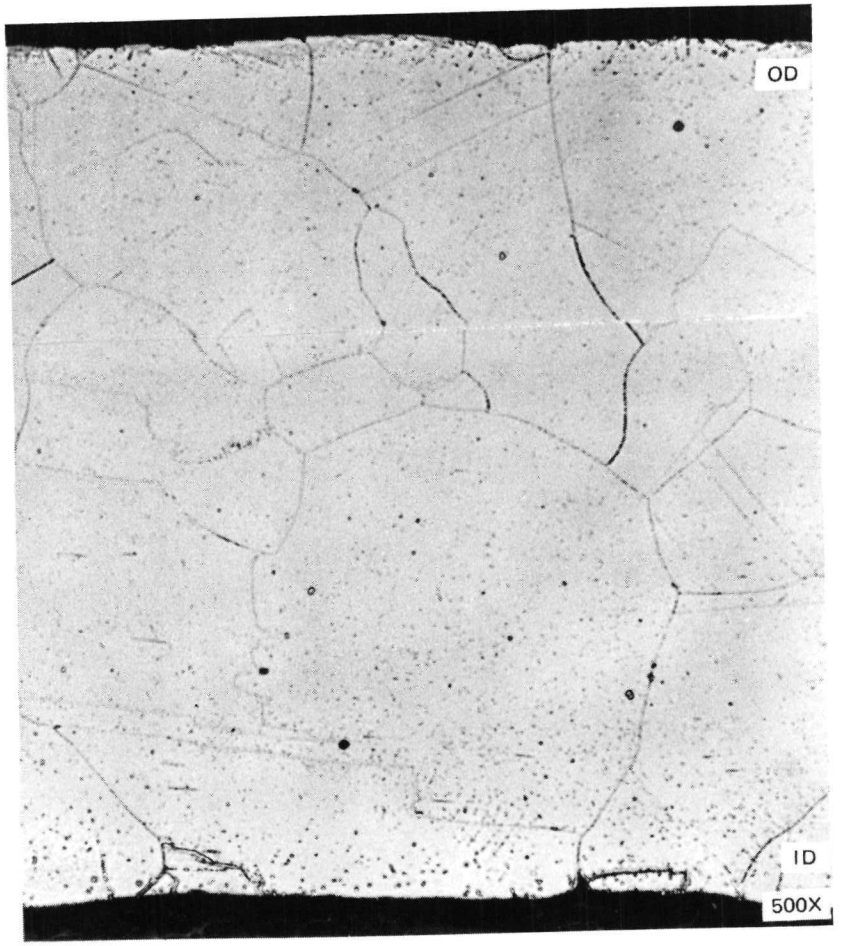

9830-3

d. 19 ksi Hoop Stress, 10.5% Diametral Strain, Not Ruptured

Figure 24. Microstructure of AISI Type 316 Stainless Steel Biaxial Stress-Rupture Specimens (Sheet 2 of 4)

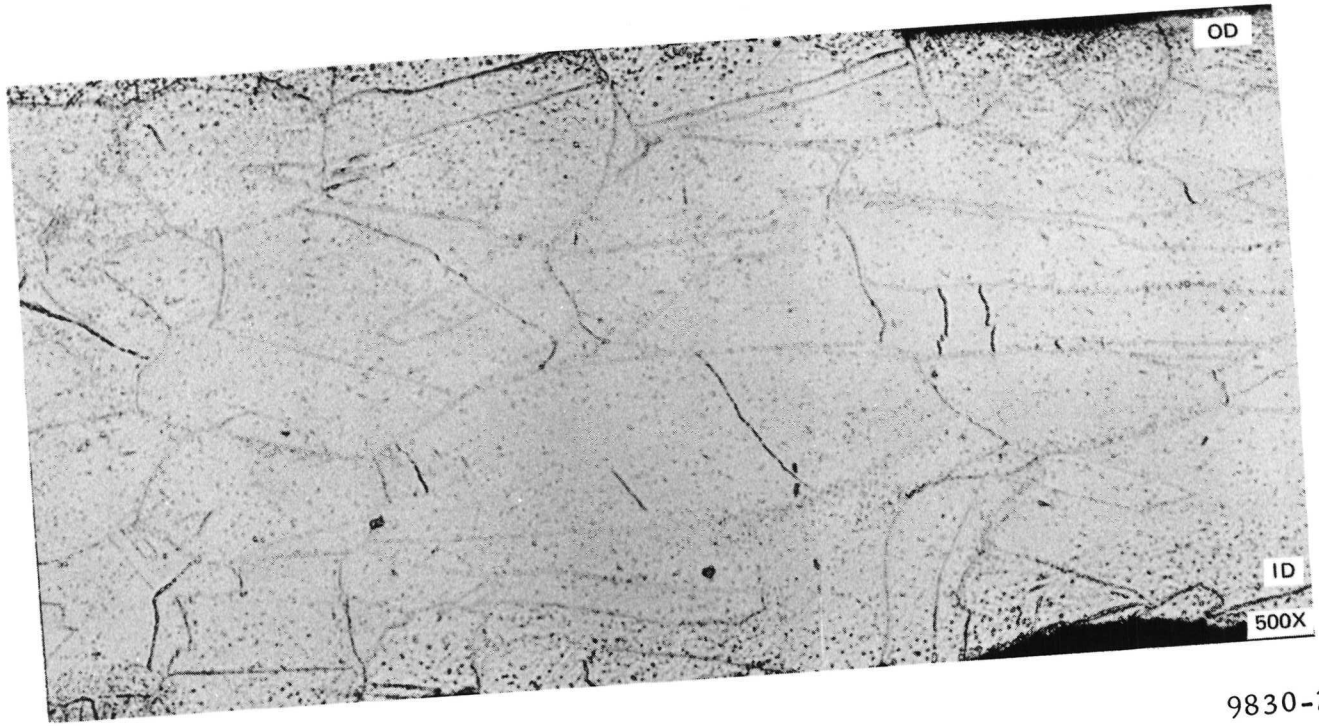

9830-2

e. 20 ksi Hoop Stress, 17% Diametral Strain, 2246-hr Rupture Time

Figure 24. Microstructure of AISI Type 316 Stainless Steel Biaxial Stress-Rupture Specimens (Sheet 3 of 4)

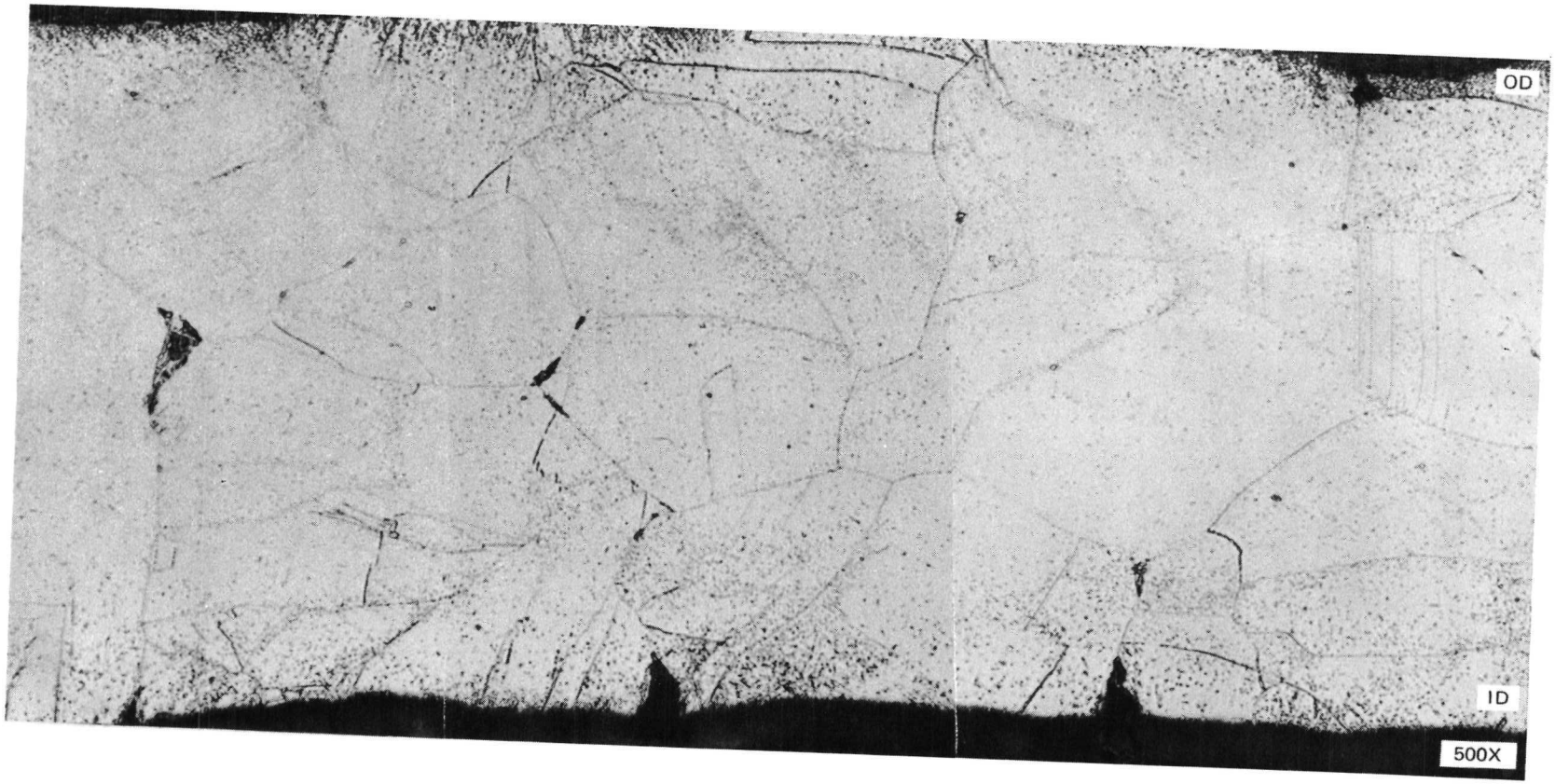

9834-2

f. 22 ksi Hoop Stress, 13% Diametral Strain, 1344-hr Rupture Time

Figure 24. Microstructure of AISI Type 316 Stainless Steel Biaxial Stress-Rupture Specimens (Sheet 4 of 4)

a strain-induced reaction than to a stress-dependent one. There does not appear to be an obvious explanation for the higher strain at rupture in the samples stressed at 20 ksi than those at 22.2 ksi. There is evidence that there is grain boundary separation and triple-point voiding in the highest-stressed sample. While the grain boundary separation is especially evident at the inside surface of the high-stressed sample, this is conspicuously absent in the 20-ksi samples. The predominant deformation mode appears to be matrix deformation. While the two predominant mechanisms may reflect the differences in strain at rupture, they do not indicate a change in material properties as a result of the exposure. It appears to be what one might expect to occur, regardless of the presence of the tantalum in the NaK.

If there had been a strength-affecting reaction, as a result of the presence of the tantalum alloy, it would have been evident in precipitation morphology, and nonuniform deformation in the ruptured samples. The preliminary carbon transport analysis summarized in Figure 20 would have indicated a significant carbon loss in at least the outer few mils of the cladding. There does not appear to be much (if any) effect. Further, there does not appear to be any corrosion or transport-inhibiting film on either the austenitic or refractory metals in the test system. Note also that a much larger Ta - 10 W:AISI Type 316 stainless steel ratio existed in these tests than would be found in the test system. This suggests that, if a reaction were to be diminished because of some test-induced variable, it would not be because there was not enough tantalum in the system to support the reactions.

These results suggest that the decarburization of the austenitic metals in the reactor system, such as the piping, may not take place as fast as had been initially anticipated. The diffusion analysis performed to date, including especially the empirical constants, should be strengthened to verify this conclusion. That is, since there is a difference between the experimental results and those predicted by the analysis, and there was no specific reason uncovered for the cause of the difference, caution should be used in interpretation of the results until they can be confirmed independently. There is nothing to indicate that this condition was due to a test-induced variable, and may not be found in a reactor system.

Although test time was limited, it is predicted, on the basis of the examination at 3000 hr, that the stress-rupture strength of the long-term, 10,000-hr sample would not have been significantly affected.

III. SUMMARY

Use of a Group Va refractory metal in the primary reactor coolant introduces a material which potentially will affect, or be affected by, the reactor environment. The possible effects include: degradation of the transition joint, loss of corrosion resistance in the piping, embrittlement by exposure to hydrogen, and change in design properties, as a result of interstitial transport between structural members.

Additions of oxygen to Ta - 10 W can significantly reduce the corrosion resistance of the alloy to the alkali metal coolant. Care must be taken to assure that the alloy does not pick up oxygen from the operating environment. Analytical models have been developed to predict the life of modules in potential service environments; portions of them have been verified by actual experience. Operation of modules for over 10,000 hr established that accelerated corrosion will not occur in adequately protected modules.

There is a definite lifetime associated with elevated-temperature operation of the coextruded transition joint. Experiments on parallel and overlapping austenitic-refractory-metal system joints indicate that the life of the joint should exceed 40,000 hr at 1200°F.

Limited experiments confirmed that the mechanical properties of the tantalum alloy are affected by relatively low quantities of hydrogen. Some portion of the hydrogen in the coolant will probably go into solution in the refractory metal during reactor shutdown. Experiments indicate that the level will probably be relatively low, in the range of the as-received value, and should not adversely affect the alloy's design properties. Experimental work was terminated prior to adequate assessment and experimental confirmation of a total hydrogen-distribution analysis.

The presence of the tantalum alloy will influence the stability of the interstitial elements, carbon, oxygen, and nitrogen, in the structural metals. Calculations indicate that strength penalties may be required in the design of the stainless steel piping. Actual experiments indicate the transport rate to be lower than initially calculated. The effect on mechanical properties therefore appears diminished. (Reaction rate experiments were planned for support of this observation, but were not completed.)

The Ta - 10 W piping can be introduced into the primary 5-kwe reactor piping without significantly affecting system reliability.

REFERENCES

1. "Compact Thermoelectric Converter Summary Report," WANL-PR(EEE)-055 (May 1973)

2. R. W. Buckman Jr. and R. C. Goodspeed "Evaluation of Refractory/Austenitic Bimetal Combinations, Final Technical Report," WANL-PR-(EE)-004 (August 1969)

3. P. B. Ferry and J. P. Page, "Metallurgical Study of Niobium/Type 316 Stainless Steel Duplex Tubing," NAA-SR-11191 (January 1969)

4. R. W. Harrison, "SNAP 8 Refractory Boiler Development, Corrosion of Oxygen Contaminated Tantalum in NaK," GESP-138 (January 1969)

5. R. L. Klueh, "The Effect of Oxygen on Tantalum-Sodium Compatibility," Met. Trans., 4, 7 (1972) pp 2145-2150

6. F. F. Schmidt et al., "Investigation of the Properties of Tantalum and its Alloys," WADD Technical Report 59-13 (March 1960)

7. H. W. Savage et al., "SNAP 8 Corrosion Program Summary Report," ORNL-3898 (1965)

8. R. W. Webb, "Hydrogen Behavior in NaK-78," NAA-SR-12025 (1967)

9. E. L. Compere and J. E. Savolainen, "The Chemistry of Hydrogen in Liquid Alkali-Metal Mixtures Useful as Nuclear Reactor Coolants, NaK-78," Trans. Amer. Nuc. Soc., 8(1) (1965) 18

10. R. J. Walter and J E. Ytterhus, "Behavior of Columbium and Tantalum in Hydrogen Environments," NAA-R-RR-67-7 (September 1967)

11. E. Veleckis, "The Thermodynamic Properties of the Systems Nb-H, V-H and Ta-H," AFO SR 1107-10F5 (1960)

12. J. R. Stephens and R. G. Garlick, "Compatibility of Tantalum, Columbium, and Their Alloys with Hydrogen in Presence of Temperature Gradient," NASA-TN-D-3546 (August 1966)

13. R. J. Walter and W. T. Chandler, "Compatbility of Tantalum and Columbium Alloys with Hydrogen," J. AIAA, 4, 2 (February 1966) pp 302-307

14. J. H. Reynold, Ed., "Brookhaven National Laboratory Progress Report, Nuclear Engineering Department," BNL 823 (August 1, 1963)

15. W. J. Anderson and G. V. Sneesby, "Carburization of Austenitic Stainless Steel in Liquid Sodium," NAA-SR-5282 (September 1960)

16. "Investigation of Bimetallic Liquid Metal Systems," GMAD-3643-8 (September 1966)

17. W. T. Lee, "Biaxial Stress Rupture Properties of Austenitic Stainless Steel in Zirconium-Gettered Sodium," NAA-SR-12353 (October 1967)

18. D. F. Atkins, "Stress-Rupture Behavior of Types 304 and 316 Stainless Steel Cladding in High-Temperature Static Sodium," AI-AEC-12976 (September 1970)

NASA Supplementary Report Distribution List for
AEC Contract No. AT(04-3)-701
LERC Order Nos. C21029 and C-21030

NASA Lewis Research Center
21000 Brookpark Road
Cleveland, Ohio 44135
Attention: Martin J. Saari (15)
M. S. 60-6

NASA Lewis Research Center
21000 Brookpark Road
Cleveland, Ohio 44135
Attention: Leonard W. Schopen (1)
M. S. 500-206

NASA Lewis Research Center
21000 Brookpark Road
Cleveland, Ohio 44135
Attention: Norman T. Musial (1)
M. S. 500-113

NASA Lewis Research Center
21000 Brookpark Road
Cleveland, Ohio 44135
Attention: Librarian (2)
M. S. 60-3

NASA Lewis Research Center
21000 Brookpark Road
Cleveland, Ohio 44135
Attention: P. E. Foster (1)
M. S. 3-19

NASA Lewis Research Center
21000 Brookpark Road
Cleveland, Ohio 44135
Attention; G. Mervin Ault (1)
M. S. 3-5

NASA Lewis Research Center
21000 Brookpark Road
Cleveland, Ohio 44135
Attention: Robert E. English (1)
M. S. 500-201

NASA Lewis Research Center
21000 Brookpark Road
Cleveland, Ohio 44135
Attention: Henry O. Slone (1)
M. S. 501-6

NASA Lewis Research Center
21000 Brookpark Road
Cleveland, Ohio 44135
Attention: Donald Packe (4)
M. S. 500-201

NASA Lewis Research Center
21000 Brookpark Road
Cleveland, Ohio 44135
Attention: B. T. Lundin (1)

NASA Lewis Research Center
21000 Brookpark Road
Cleveland, Ohio 44135
Attention: B. Lubarsky (1)
M. S. 3-3

NASA Lewis Research Center
21000 Brookpark Road
Cleveland, Ohio 44135
Attention: Samuel J. Kaufman (3)
M. S. 49-2

NASA Lewis Research Center
21000 Brookpark Road
Cleveland, Ohio 44135
Attention: V. F. Hlavin (1)
M. S. 3-10

NASA Lewis Research Center
21000 Brookpark Road
Cleveland, Ohio 44135
Attention: Neal T. Saunders (3)
M. S. 105-1

NASA Lewis Research Center
21000 Brookpark Road
Attention: Report Control Office
Cleveland, Ohio 44135
Attention: A. P. Dill (1)
M. S. 5-5

NASA Scientific and Technical
Information Facility
Acquisitions Branch
Post Office Box 33
College Park, Maryland 20740 (10)

National Aeronautics and
Space Administration
Washington, D. C. 20546
Attention: P. R. Miller (3)
Code RNP

National Aeronautics and
Space Administration
Washington, D. C. 20546
Attention: D. S. Gabriel (2)
Code NS 2

Jet Propulsion Laboratory
4800 Oak Grove Drive
Pasadena, California 91103
Attention: Library (1)

National Aeronautics and
Space Administration
Geo. C. Marshall Space Flight Center
Marshall Space Flight Center,
Alabama 35812
Attention: Library (1)

NASA Flight Research Center
P. O. Box 273
Edwards, California 93523
Attention: Library (1)

NASA Ames Research Center
Moffett Field, California 94035
Attention: Library (1)

NASA Goddard Space Flight Center
Greenbelt, Maryland 20771
Attention: Library (1)

NASA Langley Research Center
Langley Station
Hampton, Virginia 23365
Attention: Library (1)

NASA Manned Spacecraft Center
Houston, Texas 77058
Attention: Library (1)

Atomics International Division
Rockwell International

P.O. Box 309
Canoga Park, California 91304